MICROWAVE ABSORPTION CHARACTERISTICS OF NANOCOMPOSITE SILICON CARBIDE-ALUMINUM OXIDE (SiC-Al_2O_3) POWDER

A DISSERTATION

Submitted in partial fulfillment of the requirements for the award of the degree of

MASTER OF TECHNOLOGY

in

NANOTECHNOLOGY

By

JITENDRA PAL

CENTRE OF NANOTECHNOLOGY
INDIAN INSTITUTE OF TECHNOLOGY ROORKEE
ROORKEE-247 667 (INDIA)

JUNE, 2010

CANDIDATE'S DECLARATION

I hereby declare that the work, which is presented in this dissertation titled, **"Microwave Absorption Characteristics of Nanocomposite Silicon Carbide-Aluminum Oxide (SiC-Al_2O_3) Powder"** in the partial fulfillment of the requirements for the award of degree of **Master of Technology** in **Nanotechnology** submitted in the Centre of Nanotechnology, Indian Institute of Technology Roorkee, Roorkee, is an authentic record of my own work carried out from May 2009 to June 2010, under the supervision and guidance of **Dr. Dharmendra Singh**, Associate Professor and **Dr. N.P. Pathak,** Assistant Professor, Department of Electronics and Computer Engineering, Indian Institute of Technology Roorkee, Roorkee.

I have not submitted the matter embodied in this dissertation for the award of any other degree.

Date: 29/06/10

Place: Roorkee

(JITENDRA PAL)

CERTIFICATE

This is to certify that the above statement made by the candidate is correct to the best of my knowledge and belief.

Date: 29/06/2010

Place: Roorkee

(Dr. N.P. Pathak)

Assistant Professor,
E&CE Department,
Indian Institute of Technology Roorkee,
Roorkee – 247 667

(Dr. Dharmendra Singh)

Associate Professor,
E&CE Department,
Indian Institute of Technology Roorkee,
Roorkee – 247 667

ACKNOWLEDGEMENT

It gives me great pleasure to take this opportunity to thank and express my deep sense of gratitude to my guides Dr. Dharmendra Singh, Associate Professor, and co-guide Dr. N.P. Pathak, Assistant professor, Department of Electronic and Computer Engineering, Indian Institute of Technology–Roorkee for their invaluable guidance throughout the period of this dissertation work. Further I am thankful to them for all the inspiration and motivation they inculcated in me.

I am obliged to the Head of Centre of Nanotechnology for creating the right infrastructure and facilities conductive to my dissertation work. I express my sincere thanks to Dr. Anil kumar, Professor, Dr. Vijaya Agarwala, Professor, Centre of Nanotechnology for their kind help and moral support throughout this dissertation work.

I am also very thankful to Head of the Department of Electronics and Computer Engineering for providing necessary facilities for this work.

The cooperation extended by the staff of advanced microwave laboratory in the Department of Electronics and Computer engineering and the staff of Thermodynamic & Kinetics laboratory of the Department of Metallurgical & Material Engineering is gratefully acknowledge. The cooperation of Mr. Abdul Haq, Mr. Ramanpal, Mr. Naresh (Centre of Nanotechnology) and Mr. Lakhan Giri, Mr. Rajaram (Advanced Microwave Lab) for helping me during the experimentation.

My special sincere heartfelt gratitude to my family, whose sincere prayer, best wishes, support and unflinching encouragement has been a constant source of strength to me during the entire work.

Finally I would also like to thanks all my friends and classmates for their support and valuable suggestion.

Jitendra Pal

ABSTRACT

In this dissertation work, SiC-Al_2O_3 composite powder was prepared by sol-gel method for the application to lightweight microwave absorbers, which were characterized by scanning electron microscopy (SEM), X-ray diffraction analysis (XRD) respectively. The results show that, the powder obtained consists of particles of which are composed of SiC and Al_2O_3 microcrystal with the grain size of approximately 80 nm. The variation of its microwave permittivity was investigated in the frequency range of 8-12 GHz using open circuit-short circuit method and absorption were calculated using absorption testing device (ATD) for different ratio of carbon in SiC-Al_2O_3 by varying thickness. The maximum reflection loss for the composite powder was obtained -22.67 dB with a thickness of 1.2 mm.

TABLE OF CONTENTS

LIST OF FIGURES

CHAPTER 1

INTRODUCTION

1.1 Overview

Radar, developed during the Second World War, played a major role in protecting Britain (and others) from air attack. It works by transmitting bursts of radio-frequency waves that are reflected back by objects in their path. The radar antenna measures the time it takes for the reflection to arrive back, from which the distance and speed of the object are computed.

Technology on the microwave absorbers in GHz frequency band is a great topic in the military field to reduce the radar cross section (RCS) [1–4], as well as in the telecommunication engineering fields. The microwave absorber is a specially designed material to suppress the reflected electromagnetic energy incident on the surface of the absorber by dissipating the magnetic and/or electrical fields of the wave into heat. The dissipation occurs when the microwave infiltrating the structure of absorber is attenuated by lossy characteristics of the absorber. The microwave absorbers can be categorized into magnetic and dielectric absorbers according to their lossy fillers. The magnetic absorbers have been fabricated to be coating materials or flexible sheets by mixing rubbers or polymeric resins with magnetic fillers like spinel ferrites, hexagonal ferrites and/or metallic magnetic materials, etc [5–8]. The magnetic fillers are used to control both complex permeability and complex permittivity. These magnetic fillers are compounds of relatively heavy metals or ceramics and mostly used at high mixing ratios, so that most of the magnetic absorbers have high aerial weight. This is resulted from low complex permeability of magnetic fillers in GHz frequency bands. The dielectric absorbers utilize conductive fillers like nanocomposites are used to control the complex permittivity. These nanocomposites are relatively of low density and their mixing ratios are very low in comparison with those of the magnetic fillers.

The microwave absorbers for RCS reduction are usually used in external surface of structure, so that they need to have good characteristics such as light weight, thinner thickness, high structural strength and chemical resistance, as well as good absorbing performance. The nano composites

can be a good candidate for the microwave absorbers, because of its good structural and chemical performance, low dielectric constant and capability to be absorbent.

Since the nano composites show high strength, high toughness, and good thermal shock resistance, they have become one of the most promising ceramic materials with many applications, particularly at elevated temperatures. Therefore, in the past two decades, an extensive attention has been paid on fiber-reinforced nano composites because the high-quality fibers could prevent the composites' disaster failure. A substantial research effort was focused on the SiC/Al_2O_3 nanocomposite, and its excellent mechanical properties were ascribed to the presence of carbon-rich layer between the SiC and Al_2O_3. Now it is well known that the interface between fiber and nano composites plays a critical role in toughing the composites. From this point of view, the effect of the interface layer between the fiber and the matrix of a composite on mechanical properties of composites is clearly understood. But very little information is available on the effect of interface on composite's dielectric properties. However, the interface layer between oxide and carbide does exist sometimes and has strong effect on the dielectric properties [9] and [10]. E. Mouchon and P.H. Colomban [11] reported that the high conductivity of the composite SiC_f/Nasicon is mainly due to the carbon-rich fiber "crust" resulting from the degradation of the SiC Nicalon fiber. We exert effort to develop high-temperature radar wave absorbing materials (RAMs) that not only can undergo high thermo mechanical stress, but also can have high microwave absorptivity. For this application, nanocomposite is an excellent candidate. In comparison with cermets, non-magnetic ceramics with fairly stable permittivity and unchanged permeability ($\mu'=1$, $\mu=0$) ensure the designed and prepare RAM keeps constant microwave absorptivity from room to high temperature. The high imaginary parts of the permittivity and permeability are absolutely necessary for radar wave absorbing materials [12]. For the dielectric composite, $\mu'=1$, $\mu=0$, our goal, therefore, is to obtain the composites with high imaginary part of the permittivity. We found during our research that the interface layer between radar absorber, nanometer SiC, and Al_2O_3 helps to increase the imaginary part of the $SiC\text{-}Al_2O_3$ nanocomposite. This work presents our research on $SiC\text{-}Al_2O_3$ nanocomposite to show the effect of interface layer on composite's dielectric properties.

1.2 Brief Overview

Because of their great expectation in both commercial and military applications, such as electromagnetic interference shielding, radar-absorbent material (RAM) and etc., microwave-absorbing materials have generated extensive research activities. A lot of materials were synthesized and studied to achieve satisfying microwave absorption properties, from traditional ferrites to recent nanomaterials (i.e., nanocomposite, carbon nanotube) . Ferrite-related absorbing materials have excellent performance in high frequency mainly due to their high magnetic loss when subjected to alternating electromagnetic fields. However, there are still some limiting restrictions for broader utilization of ferrites as microwave-absorbing materials, such as high density, instability (especially in nanosize) and difficulty of matching electromagnetism parameter.

To further improve the microwave-absorbing performance, it is desirable to use nanomaterials owing to their exceptional physical properties comparing with bulk materials. Considering the high surface-to-volume ratio, shape effect and better match of electromagnetism parameter, composites of carbon SiC-Al_2O_3 stimulated intensive interest in microwave absorption recently. Silicon carbide (SiC) is a promising wear and high-temperature material, owing to its excellent properties for high-temperature structural applications, including high stiffness and fairly good oxidation resistance at high-temperature. In addition, SiC can be utilized as lossy additive for microwave processing, which can couple with microwave efficiently. Due to the strong covalent bonding in Sic, sintering additives (AiN, $A1_20_3$ and B_4C etc) are commonly adopted to obtain well-sintered SiC ceramic materials. The characteristics, such as shape, microstructure and grain size, of the starting Sic powder and the additive powder, have great influences on the properties of SiC ceramics sintered.

In the past decades, sol-gel techniques have been utilized to synthesize ceramic composite powders successfully. It was found that, the extensive composite homogeneity and dispersion achieved through sol-gel approaches can improve both physical and mechanical properties of products [13-17].

In the present work, SiC-A1203 composite powder was synthesized by sol-gel and carbothermal reduction method. The reaction process was analyzed by XRD and thermodynamic calculations,

and the magnetic properties (complex permittivity and complex permeability) were calculated experimentally using open circuit and short circuit method. These properties were used in optimizing thickness of RAM coating and for selection of material for highest absorption with minimum thickness (Details in Chapter 3).

CHAPTER 2

LITERATURE REVIEW

In recent years, application using electromagnetic (EM) waves, especially gigahertz (GHz) regions, has significantly expanded. These bands are further apt to higher frequency regions with the development of information technology as well as electronic devices. However, so called "EM pollution'' problems, such as EM wave interference (EMI) of electronic devices and instruments, missed action in the transportation system of railways, airplanes, or medical instrument, etc., by the EM waves have appeared along with the increasing use of the EM waves in the GHz regions (18). EM absorbers are an essential part of the defence system for their contribution to survivability of air vehicles and for use as commercial products for the EMI shielding (19). The emergence of Nanoscience and Technology opened the door for new opportunities to further improve the functionality of EM absorber (20). However, the challenge of incorporating nanoparticles into the matrix of coating is to overcome the difficulty of dispersing large volumes fractions of nanoparticles into the suitable matrix without sacrificing the mechanical properties of the resulting composites (21). The use of nanoparticles in matrix system has become a subject of interest in engineering applications due to potential changes in physical properties of nanocomposites (22). These changes in properties come from two aspects of nanoparticles: increased surface area and quantum effects associated with structure of nano-dimensional particles (23). These facts can change or enhance properties such as relativity, strength, magnetic and dielectric properties etc. of nanocomposite (24).

A typical microwave absorber consists of micron size magnetic filler materials in a polymer matrix. To get optimum absorber, up to 40-60% to volume particles are loaded into the polymer. This high volume loading of magnetic particles poses two major problems: higher weight because of high density of magnetic particles and durability since loading of the particles negate the high stain characteristics of the polymer matrix (25). This is especially true when it is used in military applications such as fighter jets where every ounce of weight is critical to its performances and frequent maintenance or repair on instruments is very costly. Also it is beneficial to have a broadband characteristic to eliminate extra absorber to cover different

frequencies. However, the design of microwave absorber is limited by the inherent material properties (26).

2.1 Radar Absorbing Materials

Many engineering requirements demand a total elimination or a reduction of EM wave reflection; diffraction and scattering as they distort radio frequency communication, create ghost images in television transmissions, or reveal the location of targets of enemy (27). Under these circumstances, an ideal solution is to apply microwave absorber on certain objects on areas to eliminate or reduce the above deterrents. Furthermore, for indoor EM wave measurements, an anechoic chamber, of which the interior is usually covered with microwave absorbers, is used to provide an interference free space environment. Here these microwave absorber fulfill the purpose of simulating the free space in a confined space. Being coated with EM absorbing materials to minimize the EM interference problems, it is possible to enhance the performances of many surveillance radar systems. Especially for those systems installed at sea where they are subjected to very strong return signals from nearby objects such as masts, high buildings, bridges, electrical cables, metal wires etc (28).

2.2 History of Microwave Absorbers: Micro to Nano

Since the mild 1930's both theoretical and experimental work has been carried out on EM wave absorber (29). The first absorber to be patented was designed and fabricated at the Namaalooze Vennootschap Machineries, in Holland in 1936 (30). This was made of quartz wave resonant material in 2 Ghz region, in which carbon black was used to achieve dissipation and titania, to achieve a high dielectric constant. Purpose was to reduce the radar cross section (RCS) of the target so that enemies radar could not detect it, during the World War II, the mission for absorbers qualities. This was necessitated mainly because of the increased use of radar in battlefield. During this period USA and Germany lunched projects to implement the EM wave absorber ideas emerging from research through development and design tests and field evaluation for use in limited number of defence applications. While Germany was interested in EM wave absorber for radio camouflage, the effort in USA was primarily directed towards developing absorbers that would enhance the radar performances by reducing interfering reflection from the nearby objects (31).

Between 1941 and 1945, a coating material called " Harp" (Halpren Anti- Radar Paint) was developed in Radiation Laboratory M.I.T of under the leadership of Harpern (32). Although the HARP coating was only 0.6 mm thick, it is achieved a return loss of -15 dB in X- band range (8-12 GHz). This material was suitable for aircraft applications because of its small thickness. Small thickness was tribute to the development of an artificial high dielectric constant material such as barium titanate. The real part of the relative dielectric constant of barium titanate is about 150 at 10 GHz, the central frequency of X band. The main components of HARP were carbon carbon black, disc shaped aluminum flakes and barium titanate in a polymer matrix. Besides HARP coating, Radiation Laboratory M.I.T of also successfully developed the now well-known "Salisbury" screen absorber. This screen showed zero reflection when a 377 ohms (impedence) resistive sheet was placed in front of a metal plate at a distance of quarter wave length. Although Salisbury absorbers were effective only for normal incident waves, its absorbing mechanism motivated scientist to continue the development of EM wave absorber (33).

During II World War, the quality of anechoic chambers became very important to obtain accurate indoor measurements. Apart from the test equipment, a perfect free space environment was required for precise measurements. Therefore, wide bandwidth and high absorption performances of EM wave absorber were required. The long pyramidal shapes loaded with carbon black were developed to cover the walls of a rectangular room so as to achieve an artificial free space environment (34). From the absorbing mechanism of pyramidal shapes from absorber was developed by gradually tailoring the required effective EM properties near that of free space at the front surface to those of a dissipative medium at the back surface. From 1945-1950 these broadband absorbers satisfied most of the requirements for anechoic chamber. The broadband absorber had been developed from the knowledge of the previous art of "dummy load" design that inspired the scientists and engineers to develop a lot of typical "dummy load materials" (35).

Other dissipative component such as metal and graphite powder, iron oxide, metal wire and steel wool had also been experienced in the development of absorber. Subsequently, lots of experimental work has been conducted on various surface geometrics including pyramids, cones, hemisphere and wedges. R.W. Wright, a scientist of U.S.Naval Research Laboratory, has been one of the most successful workers in this field (36).

In the early 1950's, Emerson of the U.S.Naval Research Laboratory developed an effective broad-band absorber which could be made by dipping or spraying tiny conducting powders such as carbon black onto a base of loosely spun animal hair. Lightweight and easy-to-make were the advantage of this kind of absorbers. The sponge products company produced the first commercial product, "Spongex", in 1951. A Spongex material with 2 inch thicknesss offered a reflection loss (RL) of about -20 dB for normal incidence at the frequency range from 2.4 to 10 GHz. In the late 1950's, Emerson & Cuming Inc. Produced absorbers for anechoic chamber, higher than -40 dB RL at a wide Frequency range (37).

In the 1960's R.E. Hiatt, Head of Radiation Laboratory, University of Michigan, Ann Arbor, demonstrated significant reduction absorber thickness using magnetic ferrite as under layeres, his work was sponsored by NASA. As those happened to be days of satellite projects, the anechoic chamber had to be useful for making many types of measurement for multipurpose. The 100-400 MHz frequency region was important for tracking and telemetry. At lower frequency it is difficult to obtain the high absorbing performances. High permeability and high permittivity magnetic material contribute for high refraction index at low frequency region and reduce the thickness of absorbers. This development made it possible to obtain unto -40 dB from 100 Mhz-1 GHz (38).

In the 1970's, Japanese used magnetic ferrite to make EM wave absorbing paint and applied it on the outside wall of high buildings to reduce the ghost image on television screen. The Plessey company in UK, a renowned manufacture of EM wave absorber, developed a new generation EM wave absorber to satisfy the requirement of British Navy including camouflage and minimizing EMI. All these efforts have resulted in the development of "Stealth material" which play a significant role in the development of advanced Bomber and aircrafts as well as the development of RAM for Naval Vessels. These development have been achieved because of a synergistic approach. The reduction of the RCS of the target has been obtained by a number of methods such as adjusting geometrical shapes to reduce the reflection at certain sensitive angles and applying the RAM onto the target surfaces (39).

2.2.1 Review of Bulksized/Nanosized Microwave Absorber

EM wave absorption characteristics of materials depend on their dielectric properties (permittivity), magnetic properties (permeability), thickness, and frequency [40], [41], [42] and [43]. Previously developed dielectric and magnetic RAMs are not without their problems. Dielectric absorbers employing conductive nano-fillers require heavy matching thicknesses and narrow absorbing bandwidths (BWs). At the same time, magnetic absorbers employing metallic or ferrimagnetic micron-sized materials suffer from heavy weight and poor characteristics in frequency ranges higher than gigahertz due to the Snoek limit [44]. The enhanced EM wave absorbers must be light, thin, and capable of wide bandwidth absorption. Previous works on single-layered X-band microwave absorbers in terms of matching thickness, 10 dB absorbing bandwidths, and mixing ratios can be found in Table 1 [43], [45], [46], [47], [48], [49], [50] and [51] J.Y. Shin, H.J. Kwon and J.H. Oh, Microwave absorbing characteristic improvement by permittivity control of ferrite composite microwave absorber, J Korean Ceramic Soc 31 (1994), pp. 415–419.[52]. Dielectric type absorbers showed 10 dB BW of about 3 GHz with the very low filler contents and thickness less than 3.0 mm. Magnetic type absorbers had 10 dB BW over about 4 GHz with the very high filler contents and thickness less than 2.5 mm. On the other hand, hybrid-type absorbers employing single filler, and mixed-type absorbers employing two fillers for both dielectric and magnetic characteristics are possible candidate materials for overcoming the narrow absorption of dielectric RAMs and heavy weight of magnetic RAMs. However, complex chemical processes and uniform dispersion techniques, in addition to other manufacturing requirements, are required for hybrid-types and mixed RAMs[53].

Table 1

Reflection loss characteristics with single-layered microwave absorber types in X-band.

Type	Filler	Matrix	Mixing ratio	*d* [mm]	10 dB BW [GHz]	Ref.
Dielectric	Carbon black	Epoxy	2.0 phr	2.78	3.0 (9.0–12.0)	[43]
	CNT	Epoxy	2.0 phr	2.23	3.0 (9.5–12.5)	[43]
	CNF	Epoxy	1.5 phr	2.07	3.0 (9.1–12.1)	[43]
Magnetic	Carbonyl iron	Polychloroprene	80 wt%	1.50	3.5 (8.0–11.5)	[45]
	MnZn ferrite	Rubber	273 phr	2.55	4.5 (8.0–12.5)	[46]
	Co–Ba ferrite	Rubber	–	2.50	5.0 (8.2–13.2)	[47]
Hybrid	$CoFe_2O_4$ filled CNT	Epoxy	–	1.40	7.0 (6.5–13.5)	[48]
	Ni–N coated CNT	Epoxy	–	1.00	1.6 (8.0–9.6)	[49]
Mixed	NiZn ferrite and SCF	Epoxy	55 + 55 phr	1.57	2.5 (8.2–10.7)	[50]
	Co ferrite and graphite	Silicone	33 + 2.6 phr	1.70	2.8 (8.4–11.2)	[51]

This research focuses on the use of both dielectric and magnetic lossy materials for the development of composite microwave absorbers that are both thin and capable of broadband absorption.

2.2.2 Performances of Microwave Absorber Nanocomposites

The continuous growth of telecommunication market leads to the emergence of a huge number of radio frequency (RF) systems. In order to allow the coexistence of all those various instruments without harmful electromagnetic interferences (EMI), it is necessary to develop new shielding and absorbing materials with high performance and large operating frequency band. A wide range of applications is concerned from commercial and scientific electronic instruments to antennas and military systems [54]. In particular, Radar Absorbing Materials (RAMs) aim at

reducing the reflectivity (or detectability) of a target by canceling reflections of radar signal incident to its surface.

Nanocomposites such as fiber-reinforced composite materials have outstanding mechanical and electrical properties that their applications have been expanded to commercial products as well as military components. Using these characteristics of composite materials, researchers have studied the radar absorbing technique, so called 'Stealth' technology. The radar absorbing efficiency of composite materials is obtained from such materials that provide special absorptive properties [55], [56] and [57] .The radar absorbing structure (RAS) is such an example that satisfies both radar absorbing property and structural characteristics. The absorbing efficiency of RAS can be obtained from selected materials having special absorptive properties and structural characteristics such as multi-layer and stacking sequence [57] and [58]. In research, to develop a RAS, three-phase composites consisted of {glass fiber}/{epoxy}/{nano size carbon materials} were fabricated, and their radar absorbing efficiency was measured on the X-band frequency range (8–12 GHz). Although some of GFR (Glass Fiber–Reinforced)-nano composites showed outstanding absorbing efficiency, during their manufacturing process, undesired thermal deformation (so called spring-back) was produced. The main cause of spring-back is thought to be temperature drop from the cure temperature to the room temperature. In order to reduce spring-back, two types of hybrid composite shells were fabricated with {carbon/epoxy} and {glass/epoxy} composites. Their spring-back was measured by experiment and predicted by finite element analysis (ANSYS). To fabricate desired final geometry, a spring-back compensated mold was designed and manufactured. Using the mold, hybrid composite shells with good dimensional tolerance were fabricated.

2.2.3 Importance of SiC Based Nanocomposites Microwave Absorber

In recent years, microwave absorptive materials have attracted considerable research interest in the materials science [59] and [60] because of its widespread applications for many electromagnetic compatibility (EMC) purposes. A number of materials have been described, which are capable of absorbing electromagnetic radiation. However, the conventional absorptive materials such as metal powders and ferrites are quite heavy, which restricts their usefulness in applications requiring lightweight mass [61]. Moreover, those materials have difficulties in

increasing the permeability in GHz region because of Snoek limit for ferrites [62] or eddy current loss for magnetic metals [63].

As one of the ways to overcome these problems, the use of embedding particles (metallic, non-metallic or polymeric) in electroless deposited metals is a convenient method of preparing composite coatings, and the particles increase its mechanical and physical properties [64]. The presence of fine particles as the second phase improves the microhardness, high-temperature inertness, wear and corrosion resistance of the composite coatings [65], [66] and [67]. High wear resistance, low cost and chemical inertness of ceramic oxides, carbides and nitrides has led to their widespread use as distributed phase [68] and [69]. Within these ceramics SiC is a kind of useful electronic material, and has high-strength ceramic material with excellent corrosion and erosion resistance. The merits of SiC for high-temperature electronics and short-wavelength optical applications are compared. The outstanding thermal and chemical stability of SiC should enable them to operate at high temperatures and in hostile environments, and also make it attractive for high-power operation [70].

However, their application still suffers from several difficulties. One problem is the low wettability between ceramics and liquid metals. In order to promote wetting between them, the ceramic surface can be modified by deposition of metal coatings using different techniques [71]. So investigations have been carried out on electrodeposited composite coatings comprising of alloy matrixes dispersed with nanoparticles, e.g. Ni–Fe–nano-Si_3N_4, Co–Ni–nano-Al_2O_3, Zn–Ni–nano-SiC, Ni–P–SiC and Co–P–SiC composite coatings are attractive and have been investigated before [72] and [73]. Ni–Co alloy coatings are of importance, as they possess high-temperature wear and corrosion resistance. Moreover, the Ni–Co alloy deposition is an anomalous co-deposition and the hardness of alloy increases as long as they possess fcc lattice structure. Thus it was necessary to understand the influence of the matrix on the properties of the composites. The composite-coating is believed to combine the advantages of both Ni–Co alloy and nano-particulate SiC. One of the available report focuses on studying the variation in SiC content in a given Ni–Co alloy obtained from Watt's bath [73].

As mentioned above, a lot of research work has been carried out on the effect of operating conditions on the mechanical properties of composite coatings containing micron size SiC particles. Reports on the magnetic and microwave-absorbing properties of nano-composite

coatings are scanty. In resonant absorbers of quarter wavelength, zero-reflection can be obtained by access to wave impedance mating at the surface of the absorbing layer, which requires a proper combination of magnetic permeability and dielectric permittivity at a given thickness and frequency. Those material parameters in high frequencies can be controlled by use of magnetic metals (permittivity control by electrical property and permeability control by magnetic property) in a single-layered microwave absorber [74]. In the present work, e.g. the thin Ni–Co–P films on SiC particles were electrolessly synthesized. It was focused on understanding the influence of Co content on magnetic and microwave-absorbing properties of composite coatings. The surface morphology and structure of Ni–Co–P films on SiC particles were also investigated.

2.2.4 Comparison Study of Different Types of SiC based Nanocomposites

In literature survey I have done study of different types of SiC based nanocomposites materials in which I got different types of results. Results are following

2.2.4.1 Al/SiC Nanocomposite

This study concentrated on the role of particle size of silicon carbide (SiC) on dimensional stability of aluminium. Three kinds of Al/SiC composite reinforced with different SiC particle sizes (25 μm, 5 μm, and 70 nm) were produced using a high-energy ball mill. The standard samples were fabricated using powder metallurgy method. The samples were heated from room temperature up to 500◦C in a dilatometer at different heating rates, that is, 10, 30, 40, and 60◦C/min. The results showed that for all materials, there was an increase in length change as temperature increased and the temperature sensitivity of aluminium decreased in the presence of both micro- and nanosized silicon carbide. At the same condition, dimensional stability of Al/SiC nanocomposite was better than conventional Al/SiC composites.

2.2.4.2 Electroless Ni–Co–P-coated SiC powder

Silicon carbide particles reinforced nickel–cobalt–phosphorus matrix composite coatings were prepared by two-step electroless plating process (pre-treatment of sensitizing and subsequent plating) for the application to lightweight microwave absorbers, which were

characterized by scanning electron microscopy (SEM), X-ray diffraction analysis (XRD), vibrating sample magnetometer (VSM) and vector network analyzer, respectively. The results show that Ni–Co–P deposits are uniform and mixture crystalline of a-Co and Ni3P and exhibit low-specific saturation magnetization and low coercivity. Due to the conductive and ferromagnetic behavior of the Ni–Co thin films, high dielectric constant and magnetic loss can be obtained in the microwave frequencies. The maximum microwave loss of the composite powder less than -32 dB was found at the frequency of 6.30 GHz with a thickness of 2.5 mm when the initial atomic ratio of Ni–Co in the plating bath is 1.5.

2.2.4.3 SiC/LAS Nanocomposite

A two-layer dielectric absorber for use as high temperature radar wave-absorbing material was developed by hot-pressing nanometer SiC and LAS glass-ceramic. The complex permittivity of the hot-pressed LAS glass-ceramic and SiC/LAS composite was investigated at 8.2–12.4 GHz. Results show that the real and imaginary parts of the permittivity's of the SiC/LAS composites greatly increase as the content of the nanometer SiC powders increases. Based on the test results, a two-layer ceramic absorber composed of LAS layer and SiC/LAS layer, covering a wide frequency range was designed and prepared. Its reflectivity at 8.2–12.4 GHz is less than −6 dB.

2.2.4.4 Hot-Pressed of SiC/Si3N4 Nanocomposites

SiC/Si3N4 nanocomposites were prepared with carbon black and α-Si_3N_4 powders by hot-pressed method. The microstructure, phase composition, dielectric and mechanical properties of the nanocomposites were investigated. The relative densities of SiC/Si_3N_4 nanocomposites decreased from 99 to 86% when the carbon black content increased from 0 to 10 wt%. The X-ray diffraction (XRD) analysis shows that there are SiC crystals formed during the sintering process in the samples with carbon black. The main crystalline phase in the pure Si_3N_4 ceramic is β-Si_3N_4. The scanning electrical microscope (SEM) photographs reveal that the Si_3N_4 grains in Si_3N_4 ceramic are big and elongated. But the transformation of α-Si_3N_4 to β-Si_3N_4 is impeded in the samples with carbon black. More α-Si_3N_4 were retained in the nanocomposites with the increase of the carbon

black content. The Si_3N_4 grains in samples with carbon black are small and particulate. The reason is that the incorporation of carbon black increases the viscosity of sintering liquid and prevents the transformation of α-Si_3N_4 to β-Si_3N_4 and the growth of Si_3N_4 grain. The strength of the nanocomposites is degraded due to the addition of the carbon black. The real and imaginary parts of the permittivity and dielectric loss of the SiC/ Si_3N_4 nanocomposites all increase with the increase of carbon black content.

** I have used SiC-Al_2O_3 nanocomposite powder as a absorbing material and compare study results from above SiC based nanocomposites can be seen in chapter 4 **.

2.4 Objective

1. To study SiC based nanocomposites for preparation of SiC-Al_2O_3 nanocomposite material.

2. Characterize the property of fabricated SiC-Al_2O_3 nanocomposite material.

3. Study the SiC based nanocomposite materials role on radar absorption.

4. Testing the performances of SiC-Al_2O_3 coating for radar absorption of X band.

2.5 Statement of the Problem

In this dissertation SiC-Al_2O_3 nanocomposite have been used as a Radar Absorbing Nano material. This has been found that increase in absorption can be achieved under the SiC-Al_2O_3 nanocomposite paint layer.

The whole problem is divided in three parts

1. Preparation of radar absorbing material

2. Preparation of Absorber Paint.

3. Calculation of complex permittivity and permeability of the absorber paint.

4. Absorption using ATD.

5. Conclusion

CHAPTER 3

METHODS & MATERIALS

3.1 Classification of Microwave Absorbers

The microwave absorbers can be classified as

1. Dielectric absorbers
2. Magnetic absorbers
3. Resonant absorbers
4. Surface current absorbers
5. Hybrid absorbers

3.1.1 Dielectric Absorbing Material

In dielectric absorbers a lossy homogeneous layer is applied to the conducting plate. In these types of absorbing material have due to the imaginary part of permittivity (ε").

3.1.2 Magnetic Absorbing Material

Magnetic absorbing materials depend on magnetic losses. Magnetic loss tangent is tan δ= μ''/μ'. Materials have higher values of μ'' and μ' give greater losses. Nanocomposites have such characteristics so they are used as microwave absorbers. The advantage of magnetic material is less thickness for adequate absorption.

3.1.3 Resonant Absorbing Material

The resonant absorbers are on in which the absorber thickness is made equal to the quarter wave length of the frequency to be absorbed and backed by a perfect conductor. It offers on open circuit to the incident wave and hence absorption.

3.1.4 Surface Current Absorbing Material

The surface current absorbers depend on the induced current in the particle for absorption of incident microwave energy.

3.1.5 Hybrid Absorbing Material

The hybrid absorbers also called broad band absorbers are a combination of the above four types and is done to increase the band width and absorption peak in the required frequency band.

3.2 Flow Chart for Preparation of SiC-Al2O3 Nanocomposite Powder

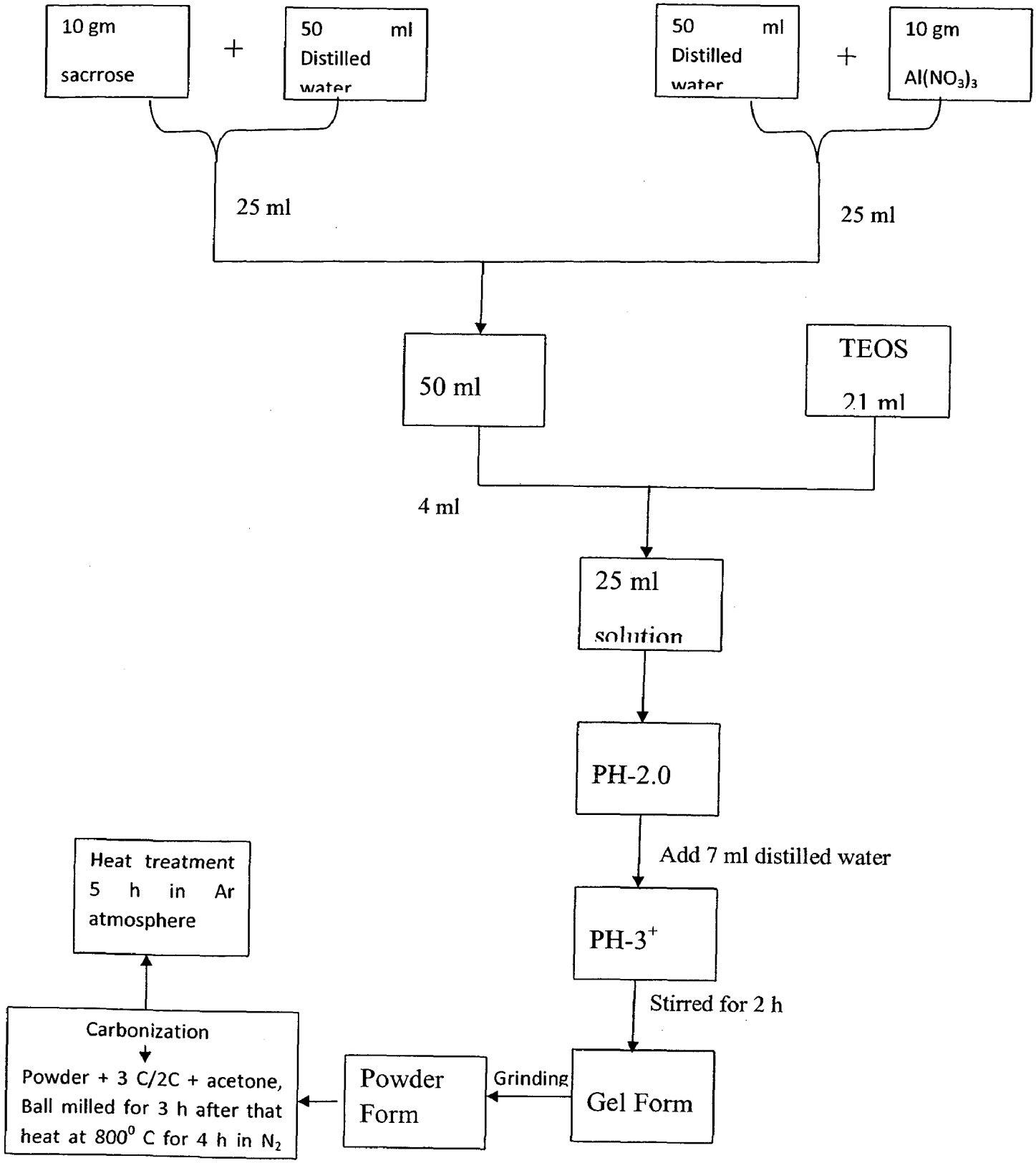

$Si0_2$-$A1_20_3$ sol with different Al / Si ratios was prepared with TEOS (tetraethylorthosilicate), A1 $(N0_3)_3$, saccharose ($C_{12}H_{22}0_{11}$), ethyl alcohol and deionized water as starting materials by the following procedures. A1 $(N0_3)_3$ and saccharose were firstly dissolved in deionized water. TEOS was mixed with the solution and agitated using magnetic stirrer at room temperature for 12 min. Then distilled water was added to adjust the mixture pH to 3-4. Finally, the mixture was further stirred for hydrolyzing for 2 h to get a transparent sol. The sol was left at 60 "C in the air until complete gelation. The xerogel of $Si0_2$-$A1_20_3$ was carbonized.

Carbonization Process

For carbonization nanocomposite powder was ball milled with fine carbon powder in acetone for 3 hours as fig 2.1 then fired at 800^0 C for 4 hours under flowing N_2 gas [75-76].

After that it was treated at 1200^0 *C for* 5 h in an argon atmosphere fig 2.2[77-81]. The phase composition of the reaction products obtained was determined by XRD (Cu target, **Ka),** and the morphology was observed by SEM.

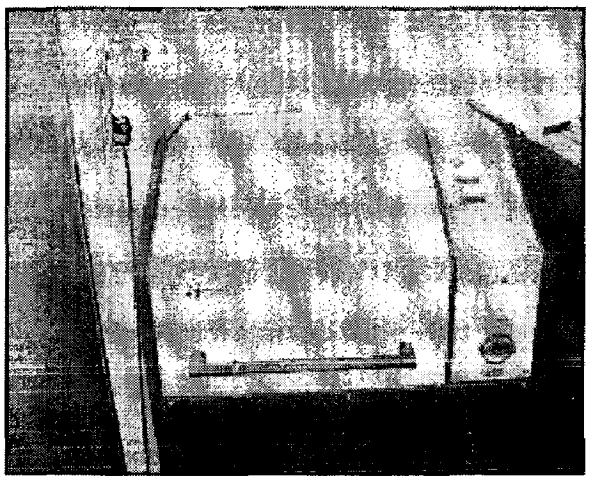

Fig 3.2.1(a) Ball milling machine

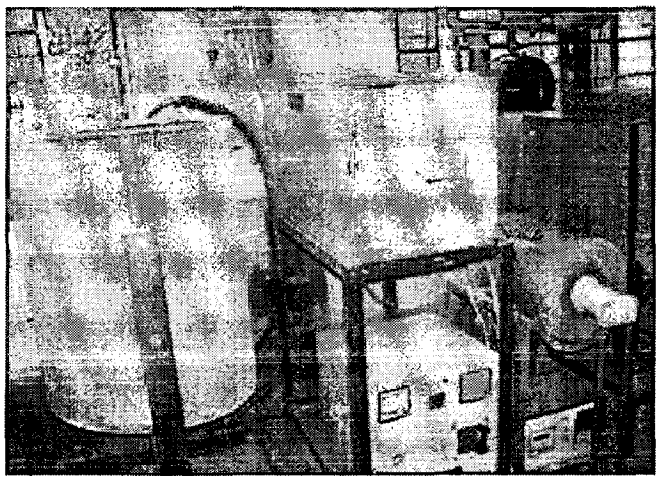

Fig 3.2.1(b) Heat treatment furnace

3.3 Selection of Binder

Various resins are commercially available but few can be used as binder to make microwave absorbing paint. We required the following properties to select a binder:

1. Excellent adhesion
2. Good thermal stability
3. flexibility
4. Good abrasion resistance
5. Excellent anti corrosive properties.

Epoxy resin (butadiene styrene) is selected as a binder because if have the all above properties. So epoxy resin is used as binder for developments of SiC-Al_2O_3 nanocomposite based absorbing paints [82].

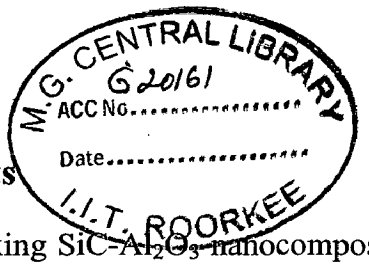

3.4 Preparation of Microwave Absorbing Paints

Microwave absorbing paints have been fabricated by mixing SiC-Al_2O_3 nanocomposite powder into epoxy resin. 40% of SiC-Al_2O_3 nanocomposite powder, 60% of an glass epoxy resin (butadiene styrene, MAT-SOL) and methyl ethyl Ketone as thinner were taken by weight. Epoxy resin is kept in oven at 110° C for half an hour, then SiC-Al_2O_3 nanocomposite powder is mixed by pastel for half an hour to generate homogeneous dispersion. Methyl Ethyl Ketone was used as thinner to achieve flow by paint. 5ml of Hardener (MAT-HARD) was mixed in 100ml paint for drying purpose. More hardener can change the properties of the paint. The paint was then sprayed by spray gun on the aluminium plates for desired thickness and cured for about 4 hours at room temperature and if required kept in oven at 60°C for half an hour. Before spray of paint, the metal plates were cleaned and roughened up by emery paper to have good adhesion [82].

3.5 Measurement of Complex Permeability and Complex Permittivity

3.5.1 Preparation of Sample

To measure the complex permeability and complex permittivity of the developed SiC-Al_2O_3 nanocomposite powder, wave-guide flange of X band have been used for the preparation of sample. The developed SiC-Al_2O_3 nanocomposite powder 40% by weight mixed with epoxy resin to from paint. The wave-guide flange was filled with developed SiC-Al_2O_3 nanocomposite paint. The wave-guide flange with paint was allowed to cure at 80°C for 6 to 10 hours. After proper curing the two faces of the flange filled with SiC-Al_2O_3 nanocomposite powder were grinded by suitable emery paper to obtain a smooth planar surfaces. The schematic diagram of the wave-guide flange containing SiC-Al_2O_3 nanocomposite is shown in figure 3.5.

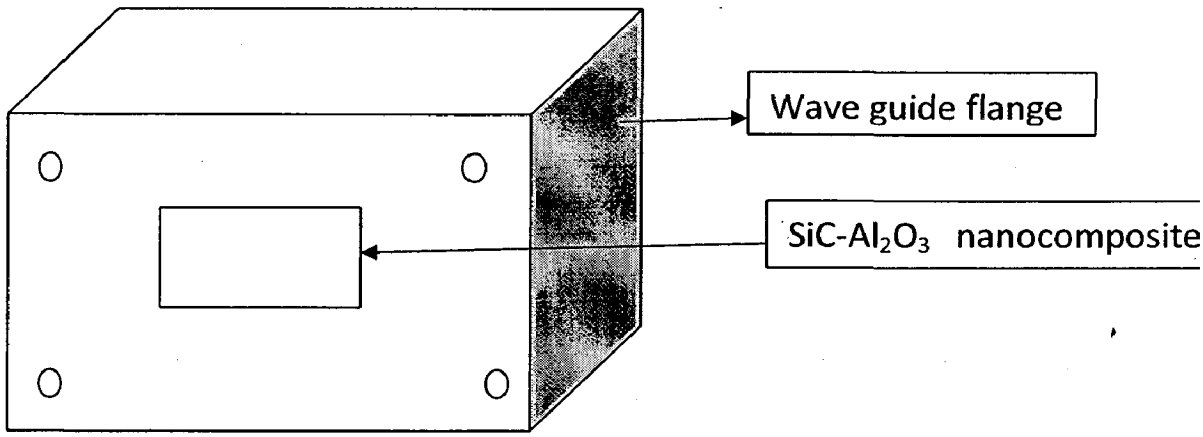

Figure 3.5: wave guide flange containing SiC-Al_2O_3 nanocomposite material for measurement of complex permeability and complex permittivity

3.6 Open Circuit and Short Circuit Method

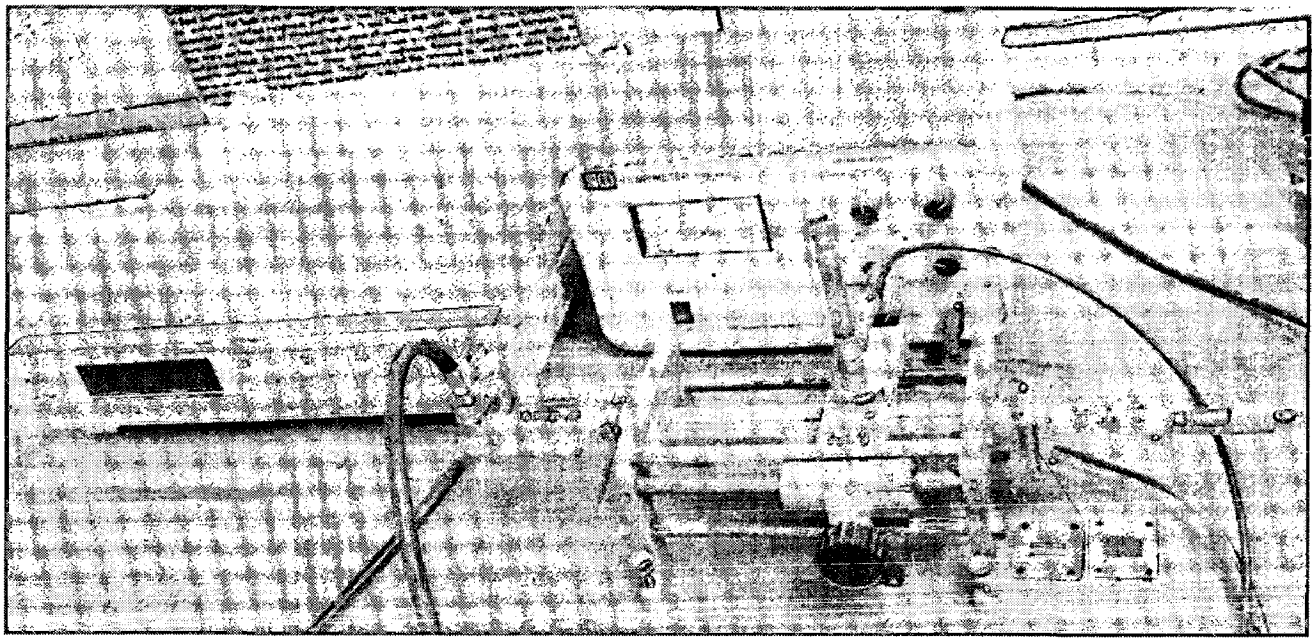

Figure 3.6(a): Experimental setup for measurement of complex permeability and permittivity of the developed SiC-Al_2O_3 nanocomposite based absorbing paint.

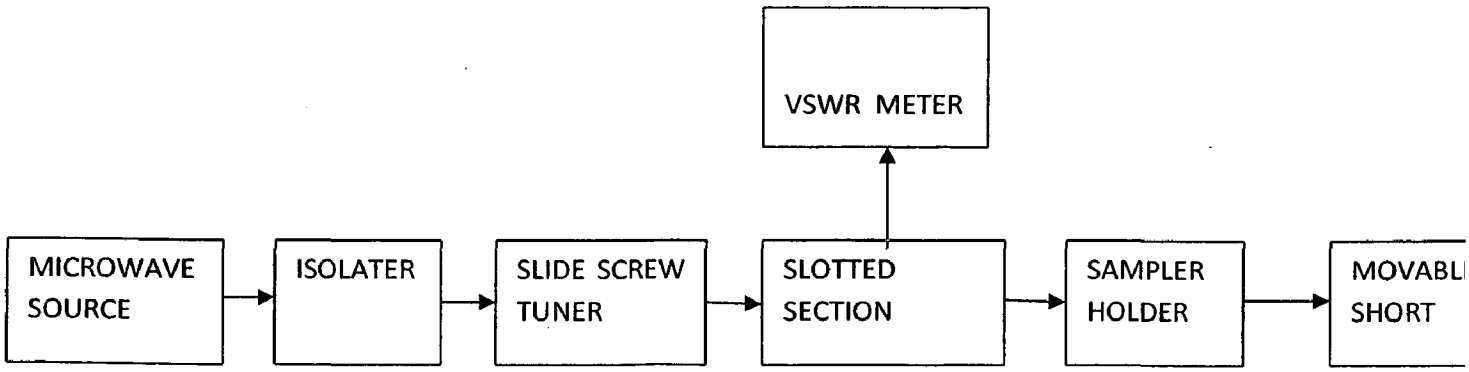

Figure 3.6(b): Block diagram of experimental setup for measurement of complex permeability and permittivity of the developed SiC-Al_2O_3 nanocomposite based absorbing paint.

The experimental setup and block diagram for measurement of complex permeability and complex permittivity is shown in figure 3.6 (b) [83]. The permeability and permittivity of each developed sample were measured experimentally.

The measurements were taken with the sample, at two different positions in the line. In one position, the field is magnetic while in the other position it is electric. For simplicity of calculation, the sample is kept in the short circuit position (predominantly magnetic) and in open circuit position (predominantly electric). The shift in minimum 'd' and voltage standing wave ration 'r' in open circuited and short circuited and short circuited condition were used for calculation of complex(μ) and values(ε).

Steps used for the measurement of shift in minima and voltage standing wave ratio (VSWR) at open circuited and short circuited condition are follows.

Step1

All the equipments were connected as shown in figure 3 the microwave source tuned to required frequency.

Step2

The guide wave length (λ_g) was obtained by measuring the distance between two minima's in the slotted line when variable short in connected to slotted line.

Step3

The wave guide flange filled with SiC-Al_2O_3 nanocomposite paint was placed and obtained d_{sc}, the position of the first minima with short touching the sample and note down the standing wave ration r_{sc} in VSWR meter.

Step4

A short was placed at a distance of $\lambda_g/4$ from the sample and determined the shift in minima d_{oc}, and note down the standing wave ration r_{oc}, under the open circuit condition.

Step5

Steps 1 to 4 were repeated over the entire band of frequency of interest.

3.7 Analysis of the data

Steps used for evaluation of complex permeability and complex permittivity are as follows:

Step 1. Wave number was determined by $k=2\pi/\lambda_g$, where λ_g is the guide wave length.

Step 2. Shift in minima 'd' and VSWR 'r' measured were used in the following equation for the calculation of admittance in short circuit in short circuit and open circuit condition and given as

$$Y_{oc} = \frac{1 + |\tau_{inoc}|e^{j2kd_{oc}}}{1 - |\tau_{inoc}|e^{j2kd_{oc}}}$$

$$Y_{sc} = \frac{1 + |\tau_{insc}|e^{j2kd_{sc}}}{1 - |\tau_{insc}|e^{j2kd_{sc}}}$$

Where

$$\tau_{insc} = \frac{r_{oc} - 1}{r_{oc} + 1}$$

$$\tau_{insc} = \frac{r_{sc} - 1}{r_{sc} + 1}$$

Where d_{sc} and d_{oc} are shift in minima and r_{sc} ,r_{oc} are the voltage standing wave ratio during short circuit and open circuit condition respectively.

Let $K_r + jK_i = \pm\sqrt{\frac{-Y_{sc}}{Y_{oc}}}$

We choose the sign of the squirt root so that K_i is positive real.

And define constant 'a' and 'b' as

$$a = 0.5\left[\tan^{-1}\frac{2K_r}{K_r^2 + K_i^2 - 1}\right]$$

And $$b = -0.25\left[\ln\frac{4K_r^2 + (K_r^2 + K_i^2 - 1)^2}{\left[(1-k_i^2)^2 + K_r^2\right]^2}\right]$$

Step 3. The relative complex permeability μ_r has been determined and is given as

$$Km = \frac{a + jb}{Kl_m}$$

$$\mu_r = \pm\left(\frac{K_m}{K}\right)[Y_{sc}Y_{oc}]^{-0.5}$$

Where I_m is the thickness of sample and μ_r is the complex permeability and given by $\mu_r = \mu_r' - j\,\mu_r''$, choose the sign($\pm$)in equation which makes the real part positive and imaginary part negative.

Step 4. The relative complex permittivity ε_r is given by [83]

$$\varepsilon_r = \left(\frac{1}{\mu_r}\right)\left\{\left[\frac{K_m}{K}\right]^2\left[1 - \left(\frac{\lambda}{2a}\right)^2\right]\right\}$$

Where 'a' is the width of the wave guide is 2.286 cm for X band.

A Matlab Program was made using to calculate the values of permittivity and permeability. Program is attached at the last of the report.

3.8 Measurement of Absorption in Developed Nanocomposite Based Absorber

The absorption of electromagnetic wave incident of on the surface of Nanocomposite based single layer absorbers have been measured by using absorber testing device methods.

3.8.1 Details of absorber testing device (ATD)

Free space condition can be defined as that condition when the impedance medium is equal to that of free space or 377 ohm. The absorber–testing device (ATD) [84] simulates the impedance conditions as required for free space. The schematic diagram of ATD is shown in figure 6.

ATD is a pyramidal horn antenna with aperture fitted to an extended wave guide terminated with a metallic variable short and having an adjustable probe as shown in the figure 6. One of the extended waveguide is fixed at the aperture of the pyramidal horn, where the end is connected to metal plate fixed with an arrangement to moving in and out. The length of the movement of the metal plate was made equal to λ_L (wave length corresponding to lowest operating frequency). A slot of length λ_L was cut in the center of the upper plate of the extended waveguide in which a movable probe is inserted to obtain proper matching.

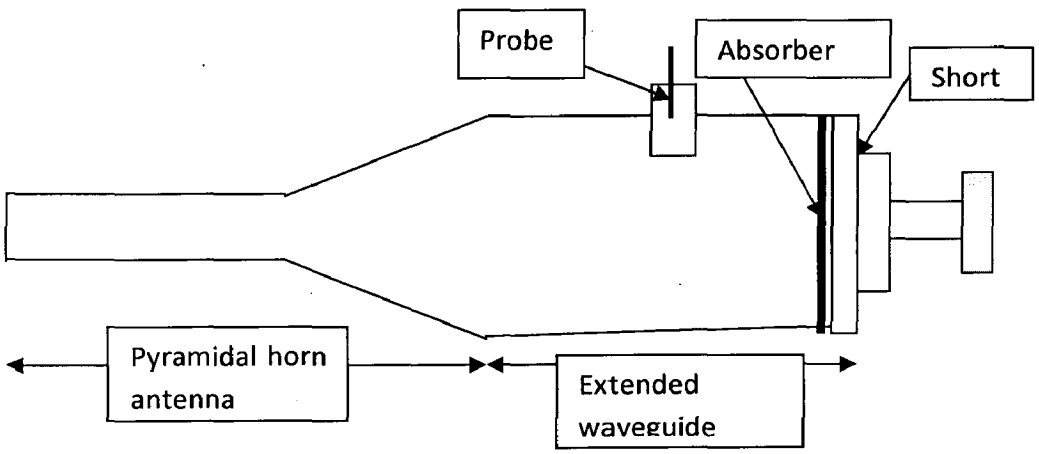

Figure 3.8.1: Schematic diagram of absorber testing device (ATD) [84]

Following assumptions are made while using ATD.

(i) Pyramidal horn being a smooth transition and does not excite any other modes.

(ii) The extended wave guide section also support the dominant TE_{10} mode.

(iii)Powers in all other modes are negligible as compared to that in TE_{10} mode.

3.8.2 Absorption measurement using ATD [82]

The block diagram of experimental setup for measurement of absorption is shown in figure 7.

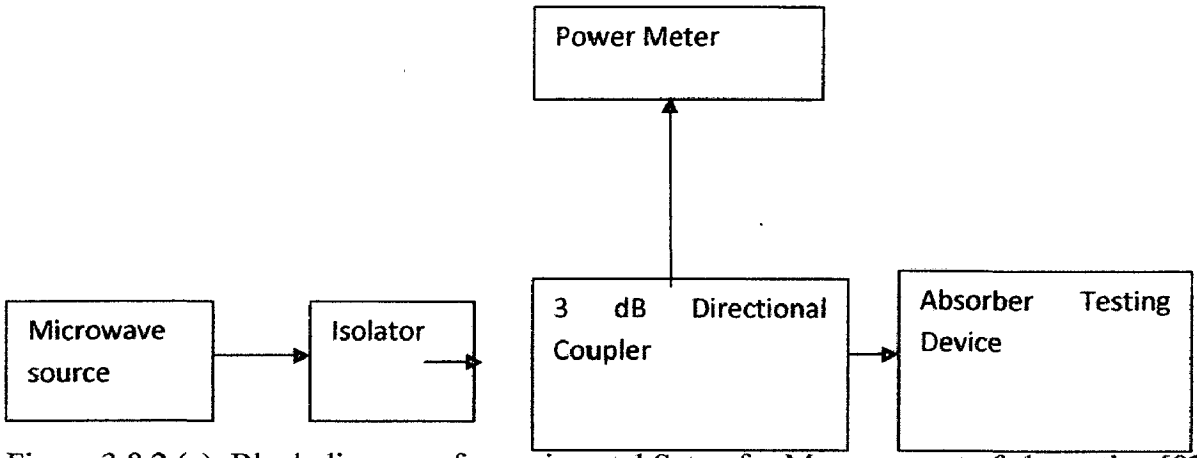

Figure 3.8.2 (a): Block diagram of experimental Setup for Measurement of absorption [82].

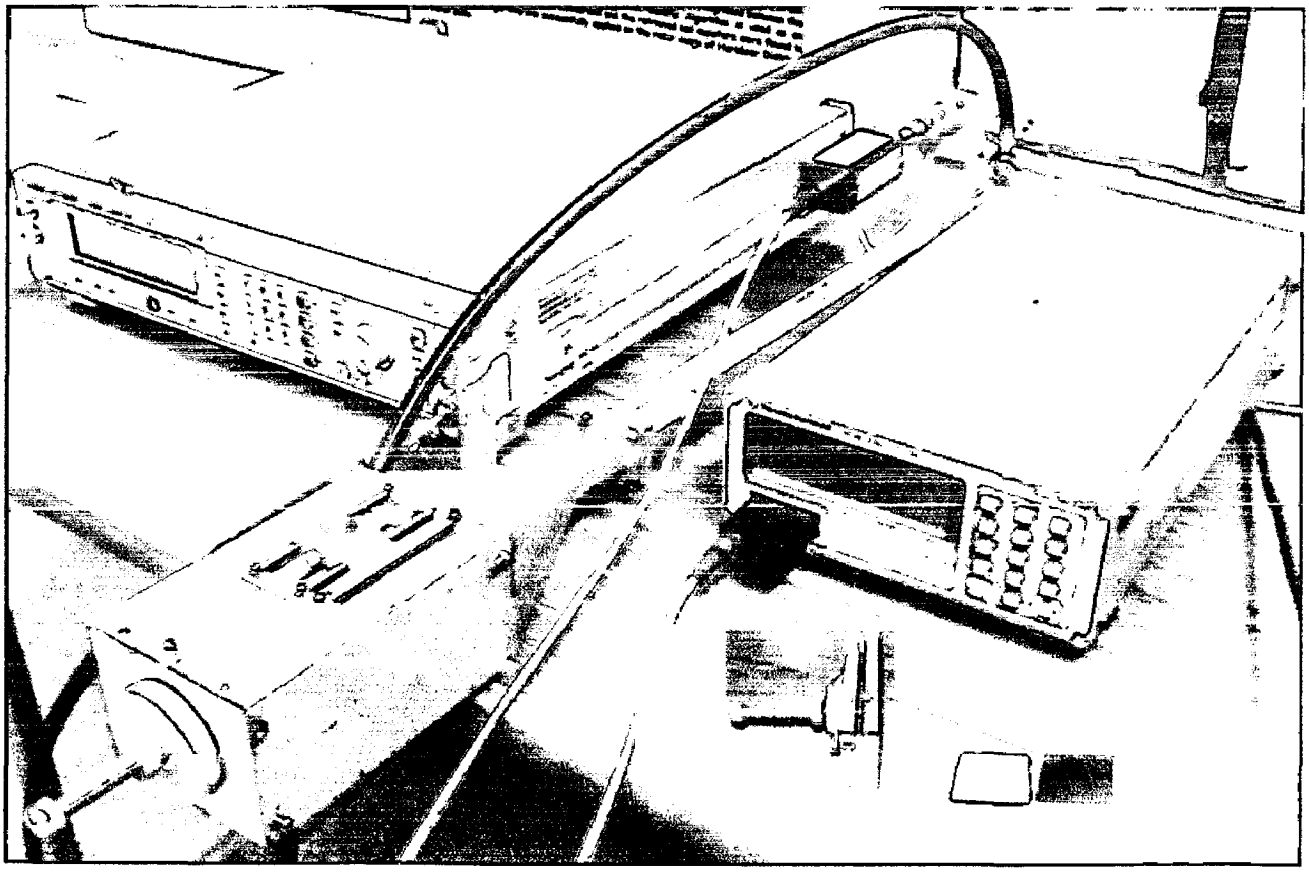

Figure 3.8.2(b): Experimental Setup for Measurement of absorption

The following steps were used for the measurement of the absorption:-

(i) All the equipments were connected as shown in figure 7 and frequency of microwave energy source was adjusted to the desired value.

(ii) A reference conducting plate of size (72.4 X 96.4 mm) was fitted in ATD.

(iii) Power meter was turned for maximum power by adjusting the position of the probe and tuner.

(iv) Reflected power (P_1) was measured.

(v) Now replacing the reference plate by an absorber plate in ATD measured the reflected power (P_2). The input powers in both the cases were kept constant.

(vi) The difference in two reading of power(P_1-P_2)gives Power Absorbed by the absorber. Thus the absorption in dB can be calculated by the following relation $Absorption\ (dB) = -10 \log_{10} \frac{P_2}{P_1}$

(vii) Step (ii) to (iv) were repeated for other frequencies of the throughout the required band of frequency.

CHAPTER 4

RESULTS & DISCUSSION

4.1 XRD and SEM/EDAX Analysis

The samples after carbonization and heat treatment in Ar atmosphere were removed from boat . Then they were analyzed separately by XRD and after that samples were analyzed by SEM /EDAX. The results of XRD analysis contained graph indicating peak values (i.e. d values) which were used to identify various phases with the help of inorganic X-ray Diffraction data card from Powder diffraction file of JCPDS. Help of software named Philips X'pert High score and Eva was also taken for finding out compounds at respective peaks.

Start Position [°2Th.]	5.0000
End Position [°2Th.]	100.0000
Settings	40 kV, 30 mA
Anode Material (Target)	Cu
Measurement Temperature [°C]	25.00
Data Origin	BRUKER-binary V3 (.RAW)
Scan Type	CONTINUOUS
Goniometer speed	2°/min

CHAPTER 4

RESULTS & DISCUSSION

4.1 XRD and SEM/EDAX Analysis

The samples after carbonization and heat treatment in Ar atmosphere were removed from boat . Then they were analyzed separately by XRD and after that samples were analyzed by SEM /EDAX. The results of XRD analysis contained graph indicating peak values (i.e. d values) which were used to identify various phases with the help of inorganic X-ray Diffraction data card from Powder diffraction file of JCPDS. Help of software named Philips X'pert High score and Eva was also taken for finding out compounds at respective peaks.

Start Position [°2Th.]	5.0000
End Position [°2Th.]	100.0000
Settings	40 kV, 30 mA
Anode Material (Target)	Cu
Measurement Temperature [°C]	25.00
Data Origin	BRUKER-binary V3 (.RAW)
Scan Type	CONTINUOUS
Goniometer speed	2°/min

4.1.1 XRD result for $SiC-Al_2O_3$ (powder + 3C) after carbonization

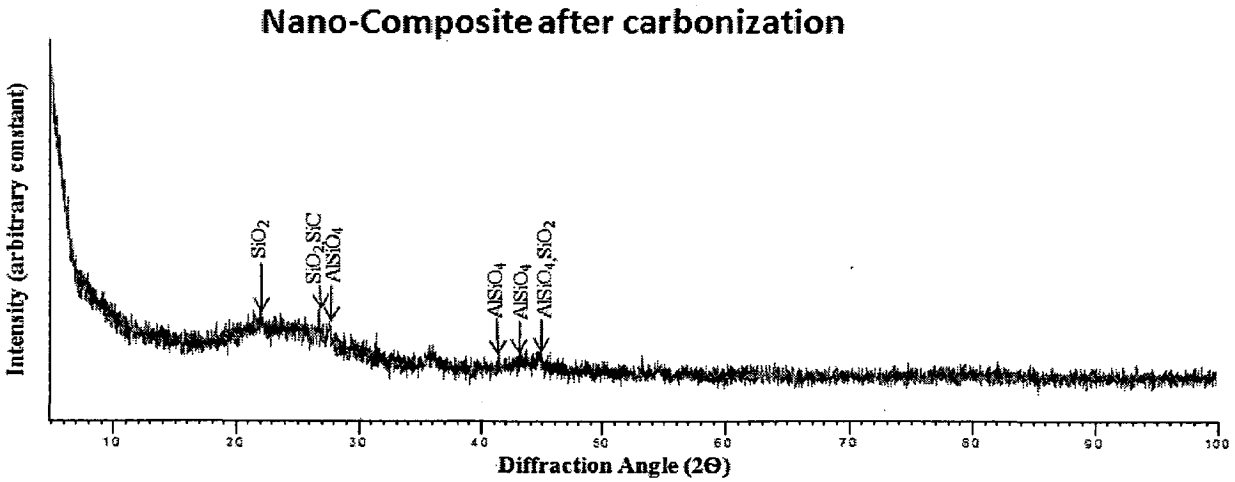

Fig 4.1.1 XRD graph for $SiC-Al_2O_3$ (powder +3C) sample after carbonization.

4.1.2 XRD result for $SiC-Al_2O_3$ (powder + 3C) after heat treatment

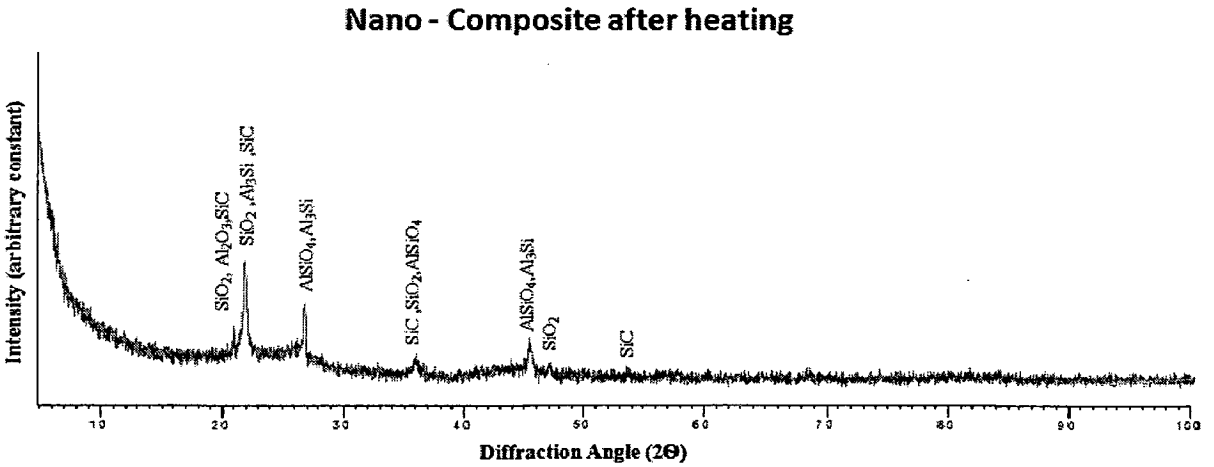

Fig 4.1.2 XRD graph for $SiC-Al_2O_3$ (powder +3C) sample after heat treatment.

From the X-Ray Diffraction analysis it is found that X-Ray Diffraction after carbonization SiO_2 {[111],[031],[222].[113]}, $AlSiO_4$ {[013],[-332],[201] are mainly formed along with SiC[113] in sample 1 and SiO_2 {[111],[220],[113]}, $AlSiO_4$ {[112],[1-20],[222]} are formed along with SiC{[113],[338],[-310]},Al_3Si {[310],[002],[312]} in sample 2 after XRD after heat treatment.

From the XRD patterns of reaction products of $SiO2$-Al_2O_3 xerogel with Al/Si atomic ratio of 15/85 are shown in Fig.4.1.1 and 4.1.2. It can be learnt that, the treating temperature has great effect on the phase composition of the products. There is no obvious peak in the pattern of the product treated at before heating in fig 4.1.1, which indicates that the powder is still composed of amorphous phases. When the treating temperature rises, there appear weak peaks indexed as mullite ($3Al_2O_3.2SiO_2$) and silicon carbide in fig 4.1.2. Accompanied by the rise of treating temperature, the peaks become intense. There exist peaks indexed as mullite, Sic and A1203 in the XRD pattern of the product obtained at high temperature. When treated at high temperature, the product obtained is composed of SiC and $A1_20_3$, and no amorphous phase can be found in the XRD pattern.

4.2 SEM Analysis

4.2.1. For SiC-Al_2O_3 (Powder + 3C) after carbonization

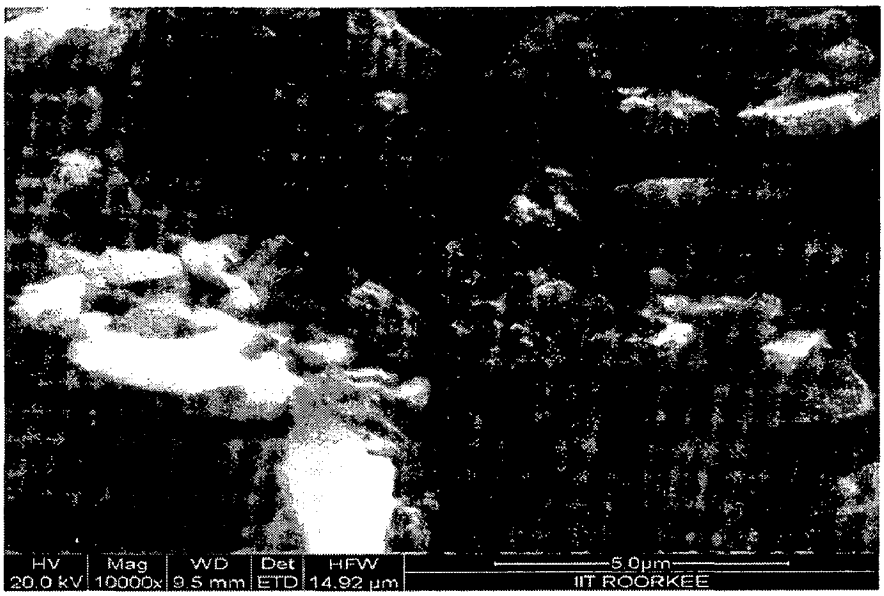

(a)

(b)

Fig 4.2.1 (a), (b) : SEM Micrograph of SiC-Al_2O_3 powder (Powder + 3C) after Carbonization

Fig 4.2.1(a), (b) shows the SEM micrograph of SiC-Al_2O_3 powder (Powder + 3C) after Carbonization. From SEM analysis it can be analysis that size to be reduced to come in nano range. In above SEM micrograph average particle size is above 100 nm.

4.2.2 For $SiC-Al_2O_3$ (powder + 3 C) after heat treatment

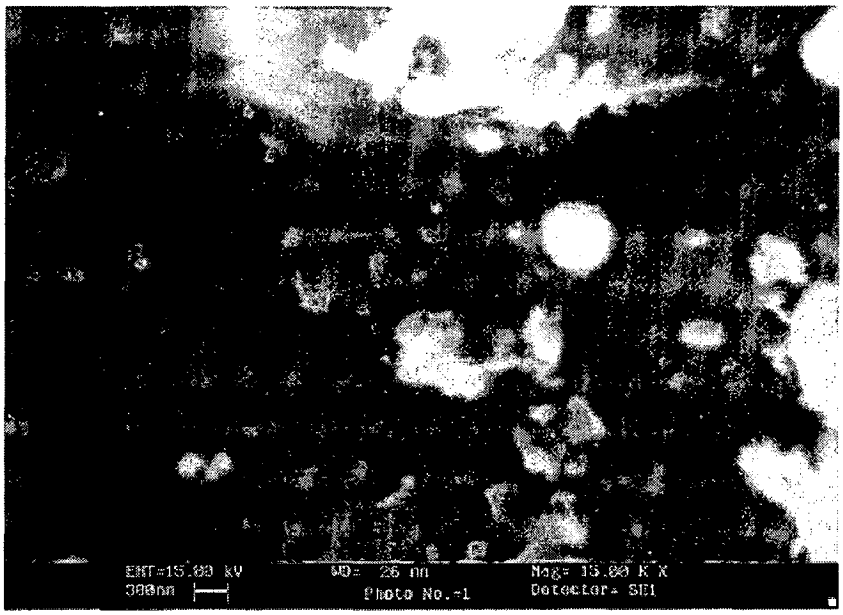

(a)

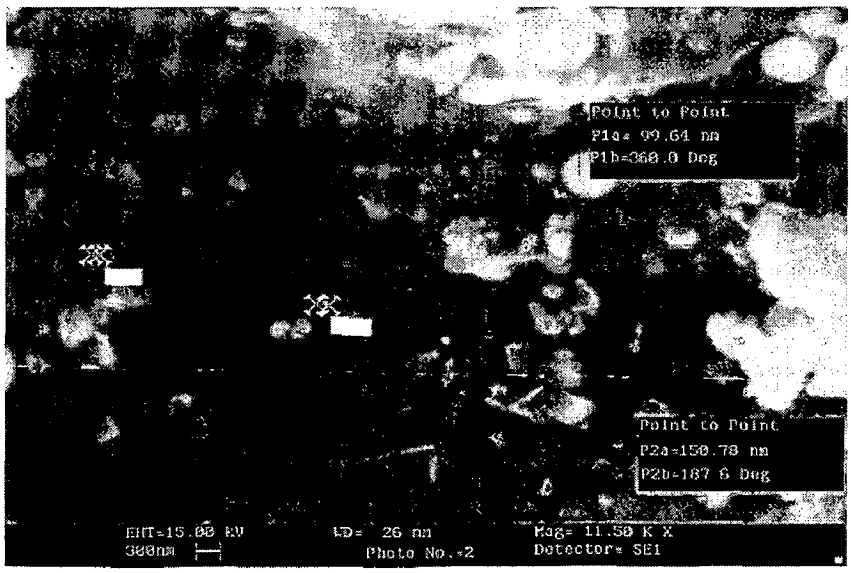

(b)

Fig 4.2.2 (a), (b): SEM Micrograph of $SiC-Al_2O_3$ powder (powder + 3C) after heat treatment

Fig 4.2.2 (a), (b) shows the SEM micrograph of $SiC-Al_2O_3$ powder (Powder + 3C) after heat treatment. From fig 4.2.1 and 4.2.2 it can be seen that treating temperature has great effect to reducing particles size. On increasing the temperature average size of the particles remains below 100 nm.

4.2.3 For $SiC-Al_2O_3$ (powder + 2 C) after heat treatment

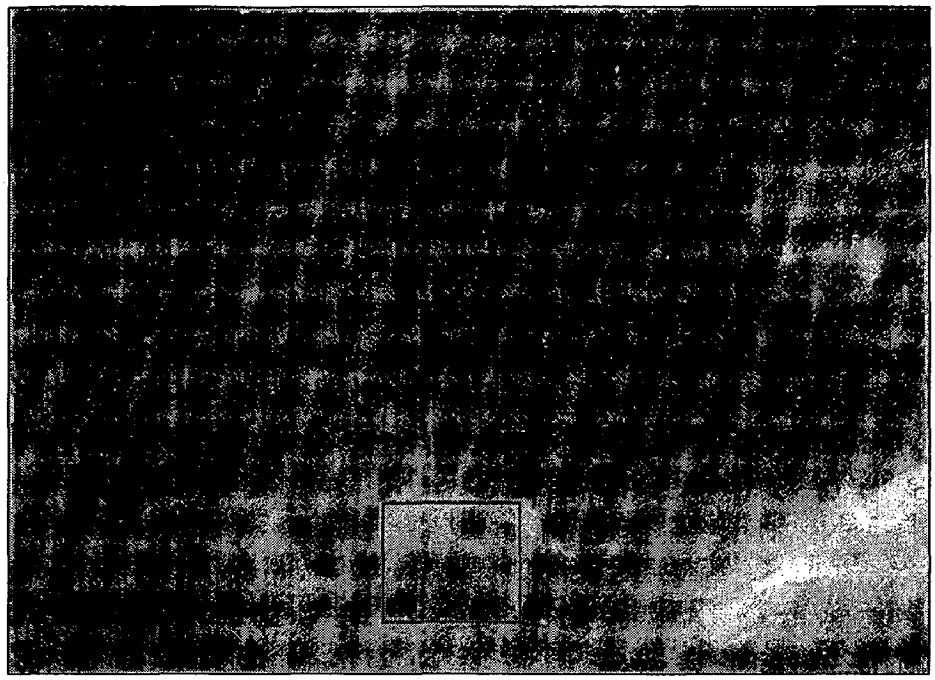

(a)

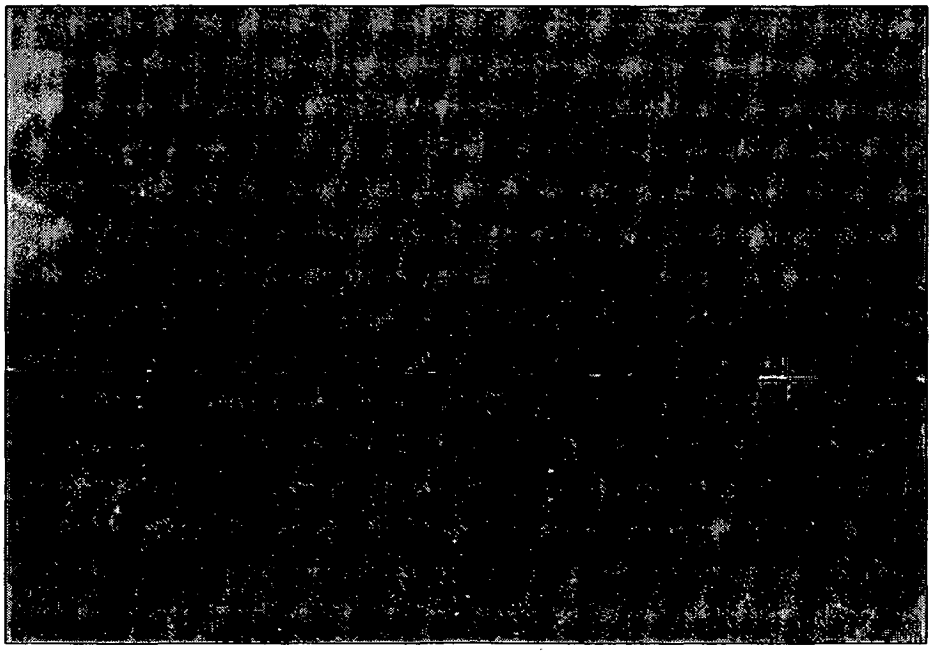

(b)

Fig 4.2.3 (a), (b): SEM Micrograph of $SiC-Al_2O_3$ powder (powder + 2C) after heat treatment

Fig 4.2.3 shows SEM micrograph of SiC-Al_2O_3 powder (powder + 2C) after heat treatment. From comparison with fig 4.2.2 and 4.2.3 it can be seen that treating temperature has great effect to reducing particles size. On increasing the temperature up to 1200^0C particles size remain in nano range (<100 nm). From analysis of SEM micrograph and EDAX analysis for powder samples after carbonization and after heat treatment as shown in Fig 4.3.1 to Fig 4.3.3, it can be seen that C and Si peak is high which shows that SiO_2 may be formed and also Al is also formed that shows oxide Al2O3 is formed along with SiC. It can be known that, A1 atoms can exist in mullite, $A1_20_3$, and amorphous phases at the treating higher temperature and also SiC can be synthesized at the higher temperature by carbothermal reduction, and the amount of SiC increases with increasing treating temperature. The reaction products of xerogel at higher temperature are the composite powder of SiC.

4.3 Results of Complex Permittivity & Complex Permeability

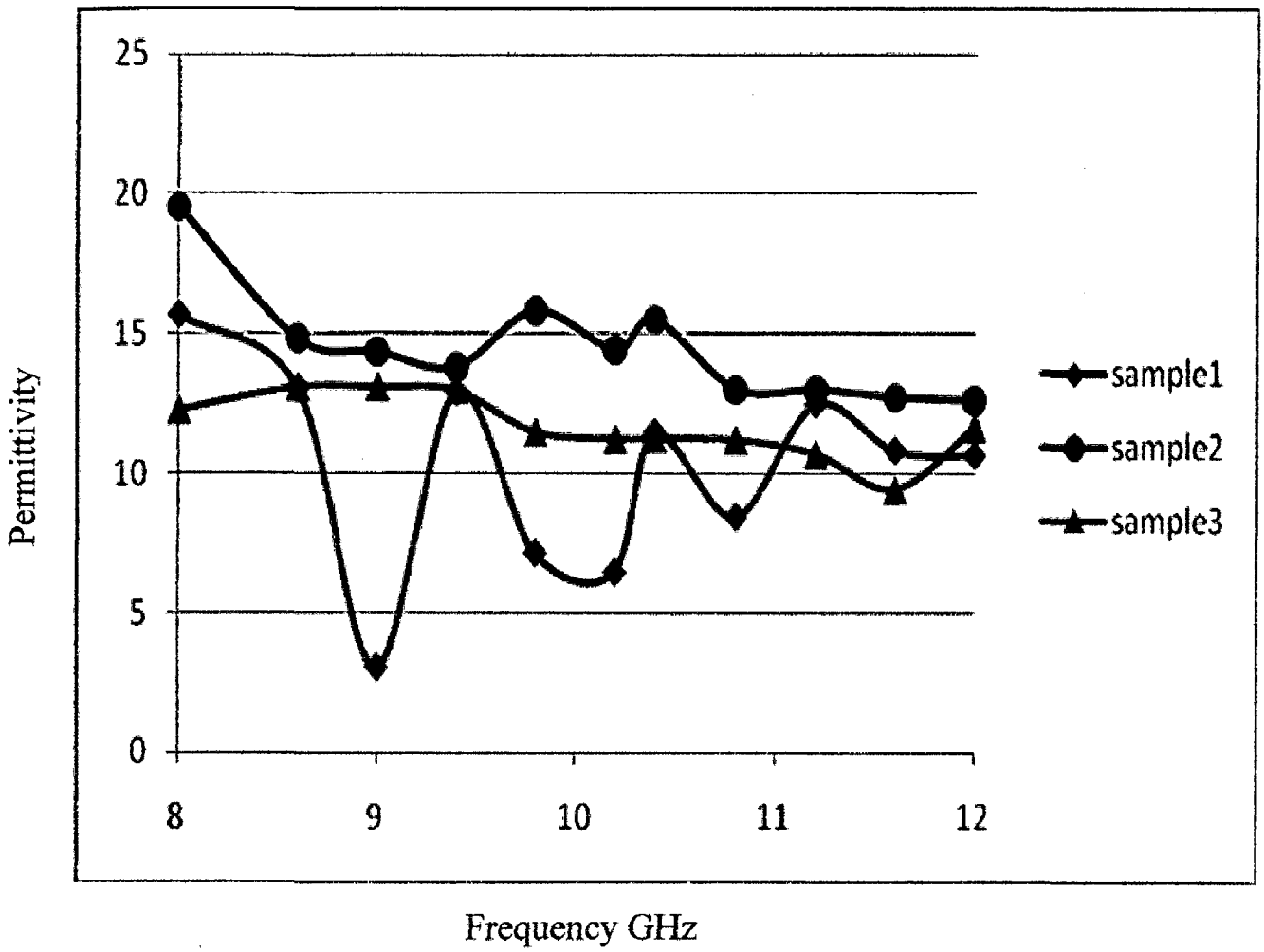

Figure 4.3 (a): Variation in real parts of the permittivity (e_r) of SiC-Al_2O_3 nanocomposite

Sample 1: Sample1 was prepared by taking ratio of SiC-Al_2O_3 (70 %) and epoxy resin (30 %). For this variation in the real part of the permittivity is varying from 15 to 10.

Sample2: Sample2 was prepared by taking SiC-Al_2O_3 (60 %) and epoxy resin (40 %). For this variation in the real part of the permittivity is varying from 19 to 11.

Sample 3: Sample3 was prepared by taking SiC-Al_2O_3 (40 %) and epoxy resin (60 %). For this variation in the real part of the permittivity is varying from 12 to 9.

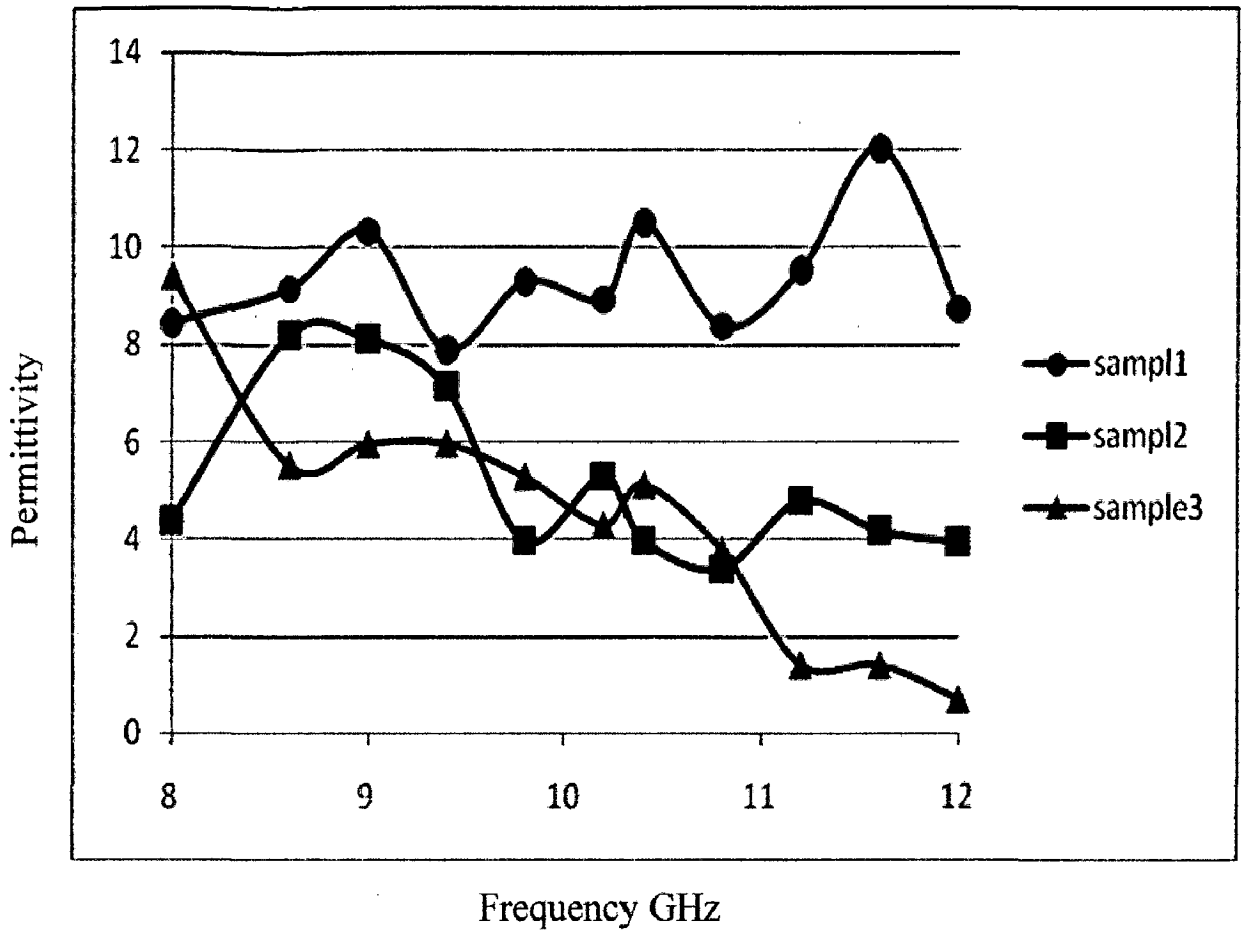

Figure 4.3 (b): Variation in imaginary parts of the permittivity (e_r) of SiC-Al_2O_3 nanocomposite

Sample 1: Sample1 was prepared by taking ratio of SiC-Al_2O_3 (70 %) and epoxy resin (30 %). For this variation in the imaginary part of the permittivity is varying from 12 to 7.

Sample2: Sample2 was prepared by taking SiC-Al_2O_3 (60 %) and epoxy resin (40 %). For this variation in the imaginary parts of the permittivity is varying from 19 to 11.

Sample 3: Sample3 was prepared by taking SiC-Al_2O_3 (40 %) and epoxy resin (60 %). For this variation in the imaginary parts of the permittivity is varying from 12 to 9.

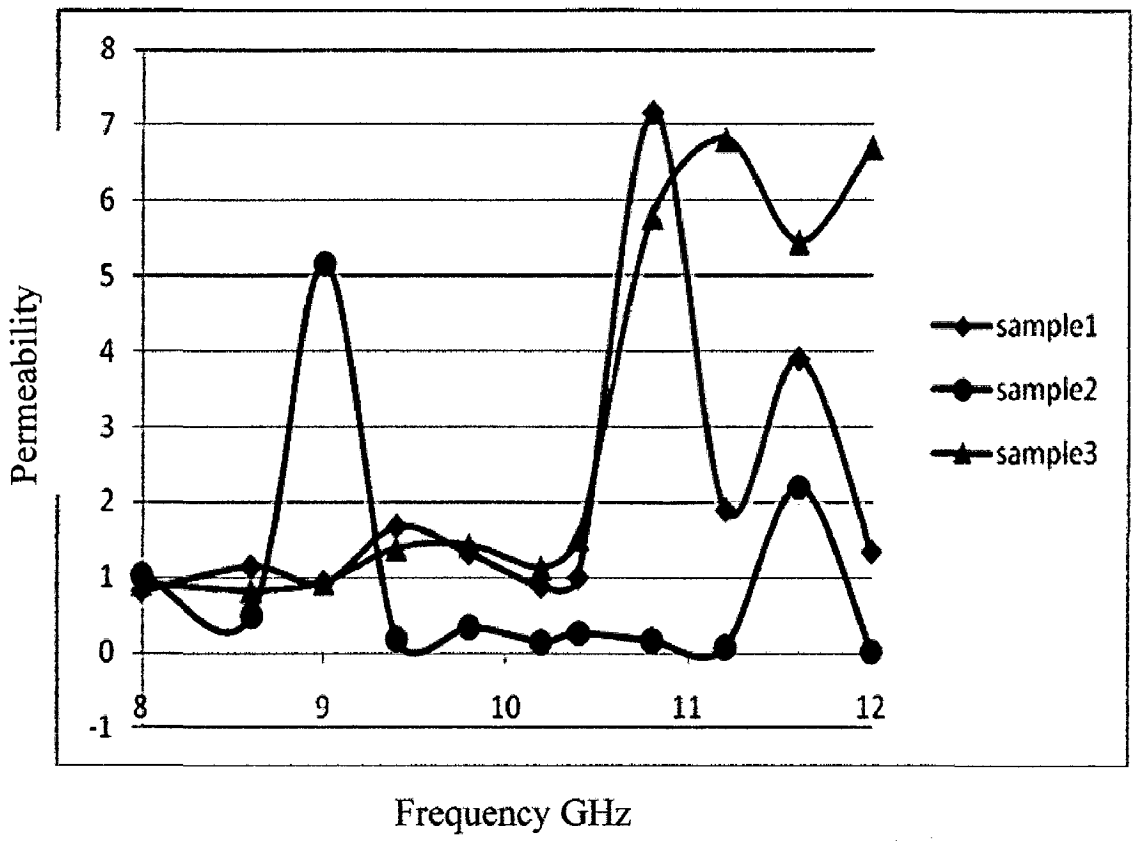

Figure 4.3 (c): Variation in real parts of the permeability (u_r) of SiC-Al_2O_3 nanocomposite

Sample 1: Sample1 was prepared by taking ratio of SiC-Al_2O_3 (70 %) and epoxy resin (30 %). For this variation in the real parts of the permeability is varying from 0.81to 7.15.

Sample2: Sample2 was prepared by taking SiC-Al_2O_3 (60 %) and epoxy resin (40 %). For this variation in the real parts of the permeability is varying from 0.0014 to 5.15.

Sample 3: Sample3 was prepared by taking SiC-Al_2O_3 (40 %) and epoxy resin (60 %). For this variation in the real parts of the permeability is varying from 0.82 to 6.71.

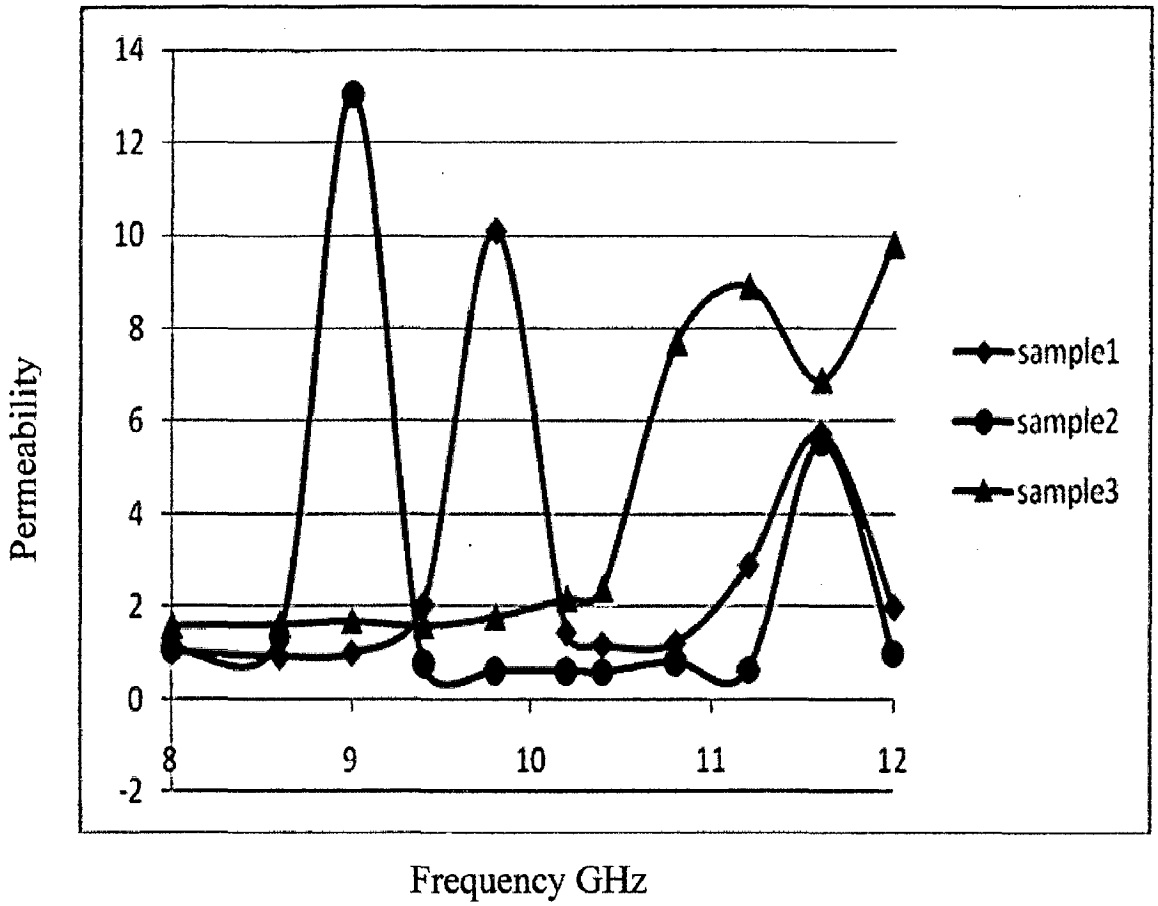

Figure 4.3 (d): Variation in imaginary parts of the permeability (u_r) of SiC-Al_2O_3 nanocomposite

Sample 1: Sample1 was prepared by taking ratio of SiC-Al_2O_3 (70 %) and epoxy resin (30 %). For this variation in the imaginary part of the permeability is varying from 0.92 to 10.

Sample2: Sample2 was prepared by taking SiC-Al_2O_3 (60 %) and epoxy resin (40 %). For this variation in the imaginary parts of the permeability is varying from 0.026 to 13.

Sample 3: Sample3 was prepared by taking SiC-Al_2O_3 (40 %) and epoxy resin (60 %). For this variation in the imaginary parts of the permeability is varying from 1.57 to 9.81.

Fig. 4.3 shows the microwave Permittivity and Permeability of the mixture of SiC-Al_2O_3 composite powder obtained in the frequency range of 8.2-12.4 GHz. According to the dielectric mixing law of polyphase materials

$$\ln\varepsilon = f_1 \ln\varepsilon_1 + f_2 \ln\varepsilon_2$$

where ε, ε_1 and ε_2 are the permittivities of composite, component 1 and component 2, respectively ; f_1 and f_2 are the volume fractions of the component phases, the complex permittivity of composite material is decided by the components.

For the powder synthesized, the main component phases are SiC, a lossy material, and Al_2O_3, a low-loss material. On account that mullite and Al_2O_3 cannot be deoxidize during the course of carbothermal reduction according to the result of XRD analysis, there is no possibility of solution of Al atoms in SiC in the way of in-situ doping.

In addition, doping of SiC cannot be performed via diffusion at higher temperature due to the strong covalent bonding in Sic. So it can be inferred that, Al atoms in the composite powder synthesized can exist only in the form of Al_2O_3, and it is impossible for Al atoms to dissolve in SiC prepared with carbothermal reduction method.

It was found that, doping of SiC induces such defects as dangling bonds and unpaired electrons, which move in response to the electric field, and lead to higher ability of absorbing microwave energy. The variation of microwave permittivity of SiC-Al_2O_3 composite powder obtained also indicates that, there is no Al atoms doped in SiC lattice.

SiC-Al_2O_3 have high dielectric constant compared to a polymer. When SiC-Al_2O_3 are mixed with the polymer, the dielectric constant of the SiC-Al_2O_3 -polymer composite will change in accordance with the filling factor. Lowering the filling factor will reduce the dielectric constant compared to the value for a pure ferrite. Characteristics behavior for the composite films in X-band frequencies for different SiC-Al_2O_3 loadings is shown in Fig. 4.3. The values of and increase with increase in the SiC-Al_2O_3 content in the polymer matrix, which is understandable because SiC-Al_2O_3 have higher values of permittivity compared to the polymer matrix.

4.4 Results of ATD

4.4.1(a) Reflection loss of SiC-Al_2O_3 (Powder + 3C) for X band

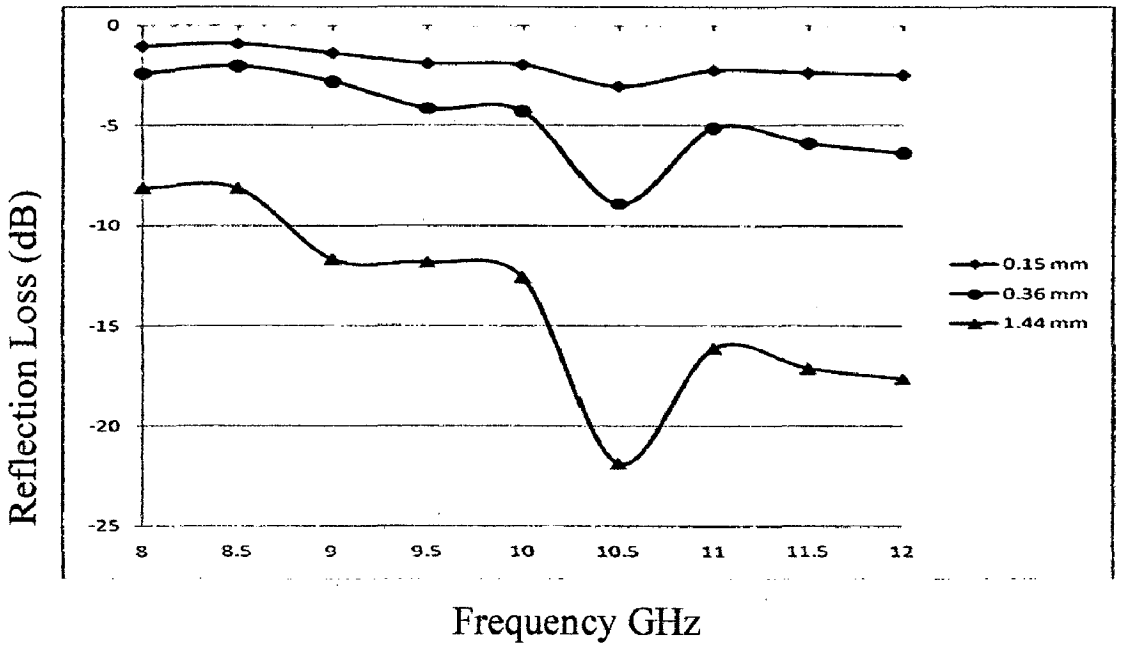

Fig 4.4.1 (a) Reflection loss of SiC-Al_2O_3 (powder + 3C) nanocomposite at different thickness for X band

4.4.1(b) Reflection loss of SiC-Al_2O_3 (Powder + 3C) for Ku band

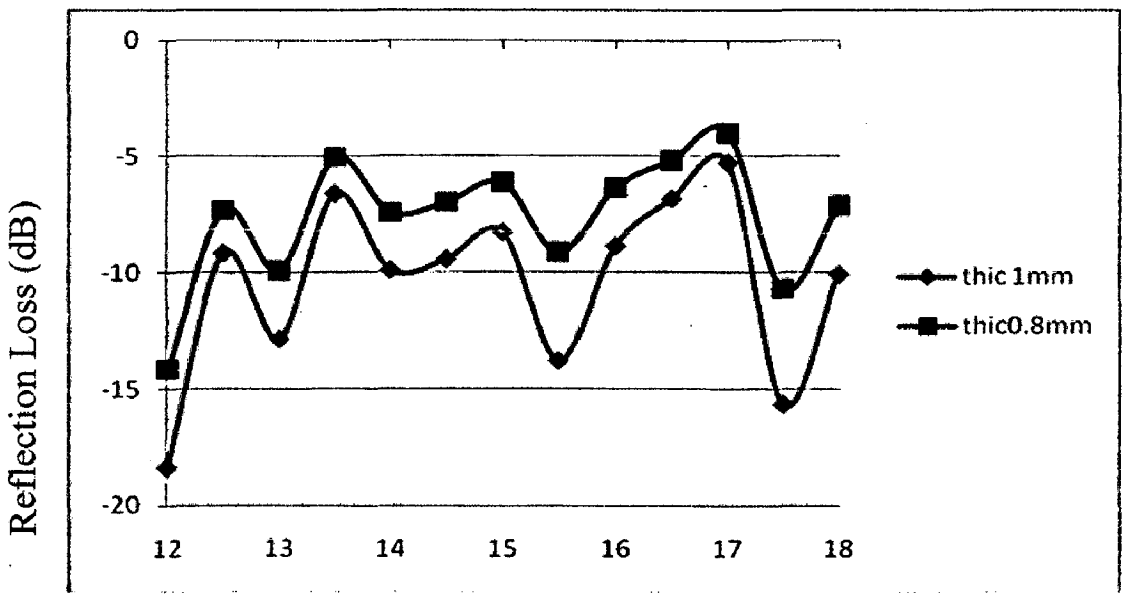

Fig 4.4.1 (b) Reflection loss of SiC-Al_2O_3 (powder + 3C) nanocomposite at different thickness for Ku band

Figure 4.4.1 (a), (b) shows reflection loss of SiC-Al_2O_3 (powder + 3C) nanocomposite at different thickness for X and Ku band. From above figures it can be seen that on increasing thickness reflection loss is increasing. Maximum reflection loss is -21.85 dB at thickness 1.44 mm for X band and for Ku band maximum reflection loss is -18.67 dB.

4.4.2(a) Reflection loss of SiC-Al_2O_3 (Powder + 2C) for X band

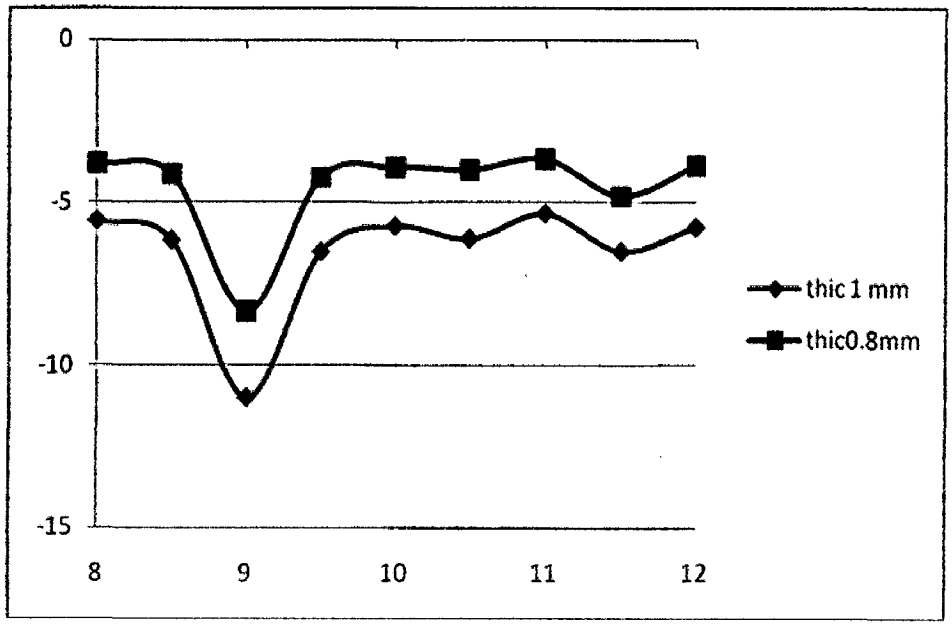

Fig 4.4.2 (a) Reflection loss of SiC-Al_2O_3 (powder + 3C) nanocomposite at different thickness for X band

4.4.2(b) Reflection loss of SiC-Al_2O_3 (Powder + 2C) for Ku band

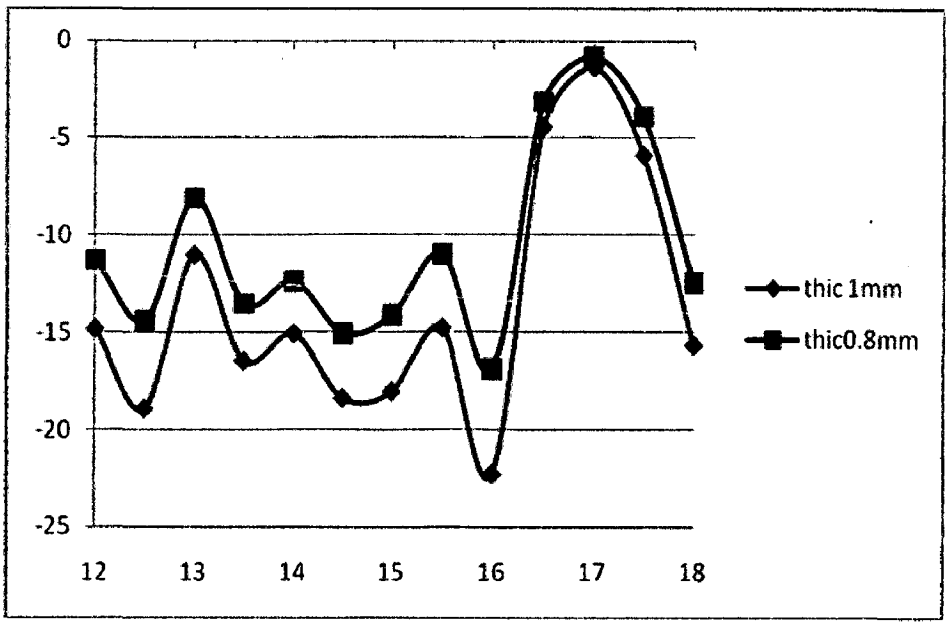

Fig 4.4.2 (a) Reflection loss of SiC-Al_2O_3 (powder + 3C) nanocomposite at different thickness for Ku band

To measure absorptive properties of SiC-Al_2O_3 for RAM reflected power was measured for frequencies of x-band at different thickness. Absorption testing device, directional coupler and frequency generator was used to measure reflected power and absorption was calculated. The 94.5 mm X 74.2 mm samples were prepared for ATD for x-band using aluminium plate.
The horn aperture was 94.3 mm X 74.2 mm. Reflection from the sample was measured direction coupler and digital power meter. One aluminium plates of the same size and thickness were used as reference plate and other was coated by SiC-Al_2O_3 nanocomposite.

The effects of the thickness of the RAM on the microwave absorption property:-

For more investigation of the microwave absorption property of the RAM, the reflectivity of the radar absorbing materials with various thickness are studied. The effects of the thickness of the RAM on the microwave absorption property are shown in Fig. 4.4.1 and 4.4.2 for X and Ku band. From the figure we can analyze that on increasing the thickness reflection loss is increasing. A maximum reflection losses of -21.85 and -18.67 dB were measured for the samples at frequency 10.5 and 12 GHz having thickness 1.44 and 1 mm for SiC-Al_2O_3 (powder + 3C) nanocomposite for X and Ku band whereas for SiC-Al_2O_3 (powder + 2C) maximum reflection losses of -11 and -22.27 dB were measured for the samples at frequency 9 and 16 GHz for X and Ku band.

CHAPTER 5

CONCLUSION

SiC-Al_2O_3 composite powder can be prepared by sol-gel and carbothermal reduction method. The powder synthesized consists of spherical particles of 100-200 nm in diameter, which is composed of SiC and Al_2O_3 microcrystal's. It can be also learnt that, the treating temperature has great effect on the phase composition of the products. There is no obvious peak in the pattern of the product treated at low temperature, which indicates that the powder is still composed of amorphous phases. When the treating temperature rises peaks will be observed. Accompanied by the rise of treating temperature, the peaks become intense. It can be also learnt from study of above results that at increasing the thickness reflection loss will be increase and maximum absorption -21.85 is obtained at thickness 1.44 mm. From study of results at different thickness we can assume that we can obtain more absorption with increasing thickness.

5.1 Future Scope

In this dissertation work SiC-Al_2O3 is used as microwave absorber which gives good absorption at small thickness. More absorption can be obtained by increasing thickness. It can be implemented with frequency selective surface (FSS) to further increase/selective absorption.

CHAPTER 6

REFERENCES

[1] M. Pardavi-Horvath, J. Magn. Magn. Mater. 215-216 (2000), pp. 171–183.

[2] Stonier RA. Stealth aircraft and technology from World War II to the Gulf (Part I: History and Background). SAMPE J 1991; 27(5): 9–18.

[3] Knott EF, Shaeffer JF, Tuley MT. Radar cross section. Norwood: Artech House; 1985.

[4] Vinoy KJ, Jha RM. Radar absorbing materials. Boston: Kluwer Academic Publishers; 1996.

[5] Naito Y, Suetake K. Application of ferrite to electromagnetic wave absorber and its characteristics. IEEE Trans Microwave Theor Tech 1971;MTT-19(1):65–72.

[6] Musal HM, Hahn HT. Thin-layer electromagnetic absorber design. IEEE Trans Magn 1989; 25(5): 3851–3.

[7] Kim SS, Jo SB, Geon KI, Choi KK, Kim JM, Kim KS. "Complex permeability and permittivity and microwave absorption of ferrite rubber composite in X-band frequencies" . IEEE Trans Magn 1991;27(6): 5462–4.

[8] Sugimoto S, Okyama K, Kondo S, Ota H, Kimura M, Yoshida Y, et al. Barium M-type ferrites as an electromagnetic microwave absorber in the GHz range. Mater Trans, JIM 1998; 39(10):1080–3.

[9] A. Jha and M.D. Moore, Glass Technology 33 (1992) (1), p. 30.

[10] Jen-Yan Hsu and R.F. Speyer, Journal of Materials Science 27 (1992), p. 374.

[11] E. Mouchon and P.H. Colomban, Journal of Materials Science 31 (1996) (2), p. 323.

[12] Philippe Colomban, Journal of Materials Research 13 (1998) (4), p. 803.

[13] SIHVOLA A. A review of dielectric mixing models[R]. Springfield: National Technical Information Service, 1997.

[14] GERSHON D L. Complex permittivity measurements and mixing laws of ceramic materials and application to microwave processing [D]. College Park: University of Maryland, 1999.

[15] BERNHOLE J, KAJIHARA S A, WANG C, ANTONELLI A, DAVIS R F. Theory of native defects, doping and diffusion in diamond and silicon carbide[J]. Mater Sci Eng, 1992, Bll(1-4): 265-272.

[16] SUZUKI M, HASEGAWA Y, AIZAWA M, NAKARA Y, OKUTANI T, UOSAKI K. Characterization of silicon carbide-silicon nitrogen composite ultrafine particles synthesized using a CO2 laser by silicon-29 magic angle spinning NMR and ESR[J]. J Am Ceram Soc, 1995, 78(1): 83-89.

[17] ZHAO D L, ZHOU W C. Preparation and microwave permittivity of nano SVCR\I composite powders suspended in different matrixes[J]. J Inorganic Mater, 2001, 16(5): 909-914. (Edited by YANG You-ping) 1939-1946.

[18] Motojima, S., Noda , Y., Hoshiya, S., and Hishikawa, Y., (2005), J. Appl. Phys., Vol.94, pp. 2325-2330.

[19] Sugimoto, S., Kondo, S., Okayama, k., Book, D., Kagotani, T., and Homma, M.,(2006), IEEE Trans. Magn. Vol. 35(5),pp. 3154-3156.

[20] Sharma, R., Agarwala, R.C., and Agarwala, V., (2006), Applied Surface science, Vol. 252, pp. 8487-8493.

[21] Vaia, R.A., and Giannelis, E.P., (2006), MRS Bulletin, Vol. 26, PP. 392-401.

[22] Jiang, K., Eitan, A., Schadler, L-S ., Ajayan, P.M and Siegel, R-W., (2006), Nano Lett., Vol.3(3), pp. 275-277.

[23] Ajayan, P.M., and Tour, J.M., (2007), Nature Materials, Vol.447,pp.1066-1068

[24] Ajayaan, P.M., (2004), Nature Nanotechnology, Vol. 427, pp. 402-403.

[25] Gindrup, W.L.,(1986), U.S. Patent No.4,624,798.

[26] Kubo, O., Ido, T., Yokoyama, H. and Koike , Y., (1985), J. Appl. Phys., Vol. 57, pp. 4280-4281.

[27] Ajayaan, P.M., (2004), Nature Nanotechnology, Vol. 427, pp. 451-453.

[28] Park, S.H., And Lee, D.N., (2006), J. Materials Science, Vol. 23, pp, 1643-1654.

[29] Gindrup, W.L.,(1986), U.S. Patent No.4,624,798.

[30] Bregar, V., (2005), IEEE Transaction on Magnetics, Vol. 40 PP. 11679- 1684.

[31] Emerson, W.H., (1973), IEEE Trans. Antenn. Propag, Vol.21(4),pp.484-490

[32] Scade, H.A., (May 1945), U.S. Tech. Mission Europe, Tech. Rep 90-45 Ad-47746.

[33] Simmons, A., Emerson, W., (July 1953), Vol. 12(7).

[34] Halpren, O., (1945), U.S Patent 2 923 934.

[35] Salisbury, W.W., (June 10, 1952), U.S Patent 2 599 944

[36] Simmons, A., Emerson, W., (July 1953), Vol. 12(7).

[37] Simmons, A., Emerson, W., (July 1953), Vol. 12(7).

[38] Wright, R.W., and Emerson, W.H., (Dec. 1954), in Pro.Con. Radio Interface Reduction.

[39] Simmons, A., Emerson, W., (July 1953), Vol. 12(7).

[40] Scade, H.A., (May 1945), U.S. Tech. Mission Europe, Tech. Rep 90-45 Ad-47746.

[41] Varadan. V.K and Varadan, V.V., (1990), US Patent No. 4, 948, 922.

[42] K.Y. Park, S.E. Lee, C.G. Kim and J.H. Han, Fabrication and electromagnetic characteristics of electromagnetic wave absorbing sandwich structures, Compos Sci Technol 66 (2006), pp. 576–584. Article | PDF (425 K) | View Record in Scopus | Cited By in Scopus (35)

[43] K.J. Vinoy and R.M. Jha, Radar absorbing materials from theory to design and characterization, Kluwer Academic Publishers, Boston (1996).

[44] K.Y. Park, S.E. Lee, C.G. Kim and J.H. Han, Application of MWNT-added glass fabric/epoxy composites to electromagnetic wave shielding enclosures, Compos Struct 81 (2007), pp. 401–406. Article | PDF (459 K) | View Record in Scopus | Cited By in Scopus (19)

[45] J.B. Kim, S.K. Lee and C.G. Kim, Comparison study on the effect of carbon nano materials for single-layer microwave absorbers in X-band, Compos Sci Technol 68 (2008), pp. 2909–2916. Article | PDF (963 K) | View Record in Scopus | Cited By in Scopus (8).

[46] J.R. Liu, M. Itoh, T. Horikawa, E. Taguchi, H. Mori and K. Machida, Iron based carbon nanocomposites for electromagnetic wave absorber with wide bandwidth in GHz range,

Appl Phys A 82 (2006), pp. 509–513. Full Text via Cross Ref | View Record in Scopus | Cited By in Scopus (11).

[47] M.S. Pinho, M.L. Gregori, R.C.R. Nunes and B.G. Soares, Performance of radar absorbing materials by waveguide measurements for X- and Ku-band frequencies, Eur Polym J 38 (2002), pp. 2321–2327. Article | PDF (282 K) | View Record in Scopus | Cited By in Scopus (46).

[48] D.Y. Kim, Y.C. Chung, T.W. Kang and H.C. Kim, Dependence of microwave absorbing property on ferrite volume fraction in Mn–Zn ferrite–rubber composites, IEEE Trans Magn 32 (1996), pp. 555–558. Full Text via Cross Ref | View Record in Scopus | Cited By in Scopus (50).

[49] S.C. Gupta, N.K. Kagrawal and C. Kumarmw, Broad band thin sheet absorbers for S- C- X- Ku-bands, J Inst Electron Telecom Eng 39 (1993), pp. 197–200.View Record in Scopus | Cited By in Scopus (8).

[50] R.C. Che, C.Y. Zhi, C.Y. Liang and X.G. Zhou, Fabrication and microwave absorption of carbon nanoutbes/CoFe2O4 spinel nanocomposite, Appl Phys Lett 88 (2006), p. 033105 (1–3). Full Text via Cross Ref | View Record in Scopus | Cited By in Scopus (29)

[51] D.L. Zhao, Y.F. Liu and Z.M. Shen, Microwave permittivity and permeability of Ni-coated carbon nanotube/polymer composites, Key Eng. Mater. 334–335 (2007), pp. 681–684. Full Text via Cross Ref | View Record in Scopus | Cited By in Scopus (2).

[52] D.I. Kim, S.M. Chung, Y.W. Park and Y. Naito, Development of microwave absorbers for X-band radar, J Korean Inst Navig 14 (1990), pp. 9–19.

[53] J.Y. Shin, H.J. Kwon and J.H. Oh, Microwave absorbing characteristic improvement by permittivity control of ferrite composite microwave absorber, J Korean Ceramic Soc 31 (1994), pp. 415–419.

[54] A. N. Yusoff, H. M. Abdullah, S. Ahmad, S. Jusoh, A. Mansor, and S. Hamid., "Electromagnetic and absorption properties of some microwave absorbers," J. Appl. Physics, vol. 92, no. 2, pp. 876–882, 2002.

[55] S. Geetha, K.K. Satheesh Kumar and D.C. Trivedi, Comp. Sci. Tech. 65 (2005), p. 973.

[56] P. Chandrasekhar, Conducting Polymers, Fundamentals and Applications: A Practical Approach (first ed.), KluwerAcademic Publishers, London (1999).

[57] A.R. Hopkins, R.A. Lipeles and W.H. Kao, Thin Solid Films 447–448 (2004), p. 474.

[58] B.J. Kim, S.G. Oh, M.G. Han and S.S. Im, Synth. Met. 122 (2001), p. 297.

[59] M.G. Han, S.K. Cho, S.G. Oh and S.S. Im, Synth. Met. 126 (2002), p. 53.

[60] R.C. Che, L.-M. Peng, X.F. Duan, Q. Chen and X.L. Liang, Adv. Mater. 16 (2004), pp. 401–405.

[61] A. Wadhawan, D. Garrett and J.M. Perez, Appl. Phys. Lett. 83 (2003), pp.2683–2685.

[62] K. Hatakeyama and T. Inui, IEEE Trans. Magn. 20 (1984), pp. 1261–1263.

[63] J. Smit and H.P.J. Wijn, Ferrites, Phillips Technical Library, Eindhoven (1959) p. 271.

[64] D. Rousselle, A. Berthault, O. Acher, J.P. Bouchaud and P.G. Zerah, J. Appl. Phys. 74 (1993), pp. 475–479.

[65] G.O. Mallory and J.R. Hajdu, Electroless Plating, AESF, USA (1990).

[66] E.A. Pavlatou, M. Stroumbouli, P. Gyftou and N. Spyrellis, J. Appl. Electrochem. 36 (2006), pp. 385–394.

[67] P. Gyftou, M. Stroumbouli, E.A. Pavlatou, P. Asimidis and N. Spyrellis, Electrochim. Acta 50 (2005), pp. 4544–4550.

[68] N.K. Shrestha, M. Masuko and T. Saji, Wear 254 (2003), pp. 555–564.

[69] K.H. Hou, M.D. Ger, L.M. Wang and S.T. Ke, Wear 253 (2002), pp. 994–1003.

[70] H. Morkoc, S. Strite, G.B. Gao and M.E. Lin et al., J. Appl. Phys. 76 (1994), pp. 1363–1398.

[71] R. Asthana, J. Mater. Sci. 33 (1998), p. 1959.

[72] R. Tarozaite, M. Kurtinaitiene, A. Dziuve and Z. Jusys, Surf. Coat. Technol. 115 (1999), pp. 57–65.

[73] L. Shi, C. Shun, P. Gao, F. Zhou and W. Liu, Appl. Surf. Sci. 252 (2006), pp. 3591–3599.

[74] S.-S. Kim, S.-T. Kim, J.-M. Ahn and K.-H. Kim, J. Magn. Magn. Mater. 271 (2004), pp. 39–45.

[75] BOULLE A, OUDJEDI Z, GWNEBRETIERE R, SOULESTIN B, DAUGER A. Ceramic nano composites obtained by Sol-gel coating of submicron powders[J]. Acta Mater, 2001,49: 81 1-816.

[76] R.KAMO, Engineered Materials Handbook, Vol.4 (ASM International, Materials park, PA, 1994).

[77] D.MOSKOWITZ // US Patent 4,108,694, August 22,1978.

[78] KENNETH J.A.BROOKES, World Directory and Handbook of Hardmetals and Hard Materials, 5th Edition (MPR Publishing Service Ltd, Old Bank Buildings, Shrewsbury SY1 1HU, England, 1981).

[79] P.F.BECHER and K.P.PLUNKNETT // J.EURO. Ceram. Soc. 18 (1997) 395.

[80] D.C. HALVERSON, K.H.EWALD and Z.A.MMUNIR // J.Mater. Sci. 28 (1993) 4583.

[81] B.L.JONG // Scripta Materialla 37 (1997) 1979.

[82] M. Meshram, Ph. D. Thesis, "Development and characterization of ferrite based microwave absorbers". Electronics and Computer Engineering Department, Indian Institute of Technology Roorkee. 2004.

[83] Gupta S. C., Agarwal N. K., and Chaitanya Kumar N. V., "Theoretical and experimental study of a single layer microwave absorber." Proceedings of National Symposium on Antenna and Propagation APSYM-92, Cochin University of science and Technology, Cochin, pp. 42-44, 29th-31st Dec 1992.

[84] Masumoto Morihiko and Miyata Yoshimori, "A gigahertz-range em wave absorber with wide band mode of hexagonal ferrites," Journal of applied Physics, Vol. 79, no. pp. 5486-5488, April 1996.

APPENDIX

Measurement of Complex Permittivity & Complex permeability

```
function p=erur % function to be called for measurement of permittivity &
                  permeability

%-------------------------------------------------------------------------%
% parametre is used for measurement of permittivity & permiablity

pi=3.14; % constant value of pi

c=3*10^10; % velocity of light

f=9*10^9

lm=0.267;  % thickness of the sample
%-------------------------------------------------------------------------%

% measurement of shift in minima & SWR

minwosp1=19.32; % first minima without sample

minwosp2=16.82; % second minima without sample


minwsp1=20.34;    % first minima with sample

minwsp2=17.82;    % second minima with sample

minwsps1=21.07;    % first minima after lemdag/4 shift with sample

minwsps2=18.62;    % second minima after lemdag/4 shift with sample

rsc=1.38;          % SWR under the short circuit condition

roc=2.2;           % SWR under the open circuit condition

dsc1=(minwosp1-minwsp1); % first shift in minima under the short circuit
                           condition

dsc2=(minwosp2-minwsp2); % second in minima under the short circuit condition

doc1=(minwosp1-minwsps1); % first shift in minima under the open circuit
                            condition

doc2=(minwosp2-minwsps2); % second shift in minima under the open circuit
                            condition
```

```
dsc=((dsc1+dsc2)/2);        % Average value of shift in minima under the short
                              circuit condition

doc=((doc1+doc2)/2);         % Average value of shift in minima under the open
                               circuit condition
%-------------------------------------------------------------------------%
%%%% above steps repeated over the entire band of frequency of interest%%%%

%-------------------------------------------------------------------------%

% measurement of wave number

lemdag=2*(minwsp1-minwsp2);

lemdag;

lemda=c/f;

k=(2*pi)/lemdag; % wave number k=2? ? ?g
%-------------------------------------------------------------------------%

% calculation of admittance in short circuit and open circuit condition

ttoc=(roc-1)/(roc+1); % reflection coefficient for open circuit

ttsc=(rsc-1)/(rsc +1); % reflection coefficient for short circuit

yoc=(1+abs(ttoc)*exp(2*k*doc*j))/(1-abs(ttoc)*exp(2*k*doc*j));   %   admittance
in open circuit Y_oc=(1+|?_inoc | e^(j2kd_oc ))/(1-|?_inoc | e^(j2kd_oc ) )

ysc=(1+abs(ttsc)*exp(2*k*dsc*j))/(1-abs(ttsc)*exp(2*k*dsc*j));   %   admittance
in short circuit Y_sc=(1+|?_insc | e^(j2kd_sc ))/(1-|?_insc | e^(j2kd_sc ) )
%-------------------------------------------------------------------------%

% measurement of The relative complex permeability & permittivity

tt=sqrt(-ysc/yoc); % Kr+jKi=±?((-Y_sc)/Y_oc )

kr=real(tt);

ki=imag(tt);

if(ki<0) % condition

    Kr=-kr;

    Ki=-ki;

else
    Kr=kr;
```

```
    Ki=ki;

End

Kr+(Ki*j);

a=0.5*(atan((2*Kr)/((Kr^2)+(Ki^2)-1)));  % constant parametre a=0.5[tan^(-
1)??(2K_r)/(K_r^2+K_i^2-1)? ] .

b=-0.25*(log(((4*(Kr^2))+(((Kr^2)+(Ki^2)-1)^2))/((((1-Ki)^2)+(Kr^2))^2)));  %
constant parametre b=-0.25[ln??(4Kr^2+(Kr^2+Ki^2-1)^2)/[(1-ki^2 )^2+Kr^2 ]^2
? ]

Km=(a+(j*b))/(k*lm);

ur=(Km/k)*((ysc*yoc)^(-0.5)); % The relative complex permeability

er=((1/ur)*((((Km/k)^2)*(1-((lemda/(2*a))^2))))+((lemda/(2*a))^2));   % The
relative complex permittivity

er

if(real(ur)<0)

ur=-ur;

end

ur
```